CrossMark
click for updates

View Article Online
View Journal

Dalton Transactions

Accepted Manuscript

This article can be cited before page numbers have been issued, to do this please use: A. FerrerUgalde, J. Cabrera-González, E. J. Juárez-Pérez, F. Teixidor, E. Perez-Inestrosa, J. M. Montenegro, R. Sillanpää, M. Haukka and R. Nunez, *Dalton Trans.*, 2016, DOI: 10.1039/C6DT04003A.

This is an Accepted Manuscript, which has been through the Royal Society of Chemistry peer review process and has been accepted for publication.

Accepted Manuscripts are published online shortly after acceptance, before technical editing, formatting and proof reading. Using this free service, authors can make their results available to the community, in citable form, before we publish the edited article. We will replace this Accepted Manuscript with the edited and formatted Advance Article as soon as it is available.

You can find more information about Accepted Manuscripts in the author guidelines.

Please note that technical editing may introduce minor changes to the text and/or graphics, which may alter content. The journal's standard Terms & Conditions and the ethical guidelines, outlined in our author and reviewer resource centre, still apply. In no event shall the Royal Society of Chemistry be held responsible for any errors or omissions in this Accepted Manuscript or any consequences arising from the use of any information it contains.

ROYAL SOCIETY OF CHEMISTRY

rsc.li/dalton

View Article Online
DOI: 10.1039/C6DT04003A

Published on 13 December 2016. Downloaded by Instituto de Ciencia de Materiales de Barcelona (ICMAB) on 22/12/2016 09:59:23.

Carborane-stilbene dyads: influence of substituents and cluster isomers on the photoluminescence properties†

A. Ferrer-Ugalde,[a#] J. Cabrera-González,[a] E. J. Juárez-Pérez,[a#] F. Teixidor,[a] E. Pérez-Inestrosa,[b,c] J. M. Montenegro,[b,c] R. Sillanpää,[d] M. Haukka and [d] R. Núñez*[a]

[a] *Institut de Ciència de Materials de Barcelona (ICMAB-CSIC), Campus U.A.B., 08193, Bellaterra, Barcelona, Spain. E-mail: rosario@icmab.es*

[b] *Universidad de Málaga, IBIMA, Department of Organic Chemistry, 29071-Malaga, Spain.*

[c] *Andalusian Centre for Nanomedicine and Biotechnology-BIONAND, Parque Tecnológico de Andalucía, 29590-Málaga, Spain.*

[d] *Department of Chemistry, University of Jyväskylä, FIN-40014, Jyväskylä, Finland.*

[#] A. Ferrer-Ugalde current address: School of Chemistry and Chemical Engineering. Queen's University of Belfast, David Keir Building, Belfast, BT9 5AG, United Kingdom; E. J. Juárez-Pérez current address: Energy Materials and Surface Sciences Unit (EMSS), Okinawa Institute of Science and Technology Graduate University (OIST), 1919-1 Tancha, Onna-son, Okinawa, 904-0495, Japan

† Electronic Supplementary Information (ESI) available: See DOI 10.1039/x0xx00000x

Dalton Transactions Accepted Manuscript

View Article Online
DOI: 10.1039/C6DT04003A

Published on 13 December 2016. Downloaded by Instituto de Ciencia de Materiales de Barcelona (ICMAB) on 22/12/2016 09:59:23.

Two novel styrene-containing *meta*-carborane derivatives substituted at the second carbon cluster atom (C_c) with either a methyl (Me), or a phenyl (Ph) group, are introduced herein alongside with a new set of stilbene-containing *ortho*- (*o*-) and *meta*- (*m*-) carborane dyads. The latter set of compounds has been prepared from styrene-containing carborane derivatives via Heck coupling reaction. High regioselectivity has been achieved for these compounds by using a combination of palladium complexes $[Pd_2(dba)_3]/[Pd(t\text{-}Bu_3P)_2]$ as a catalytic system, yielding exclusively *E* isomers. All compounds have been fully characterized and the crystal structures of seven of them analyzed by X-ray diffraction. The absorption spectra of these compounds are similar to those of their respective fluorophore groups (styrene or stilbene), showing very low influence of the substituent (Me or Ph) linked to the second C_c atom or the cluster isomer (*o*- or *m*-). On the other hand, fluorescence spectroscopy revealed high emission intensities for Me-*o*-carborane derivatives, whereas their Ph-*o*-carborane analogues evidenced an almost total lack of fluorescence, confirming the significant role of the substituent bound to the adjacent C_c in *o*-carboranes. In contrast, all the *m*-carborane derivatives display similar photoluminescence (PL) behavior regardless of the substituent attached to the second C_c, demonstrating its small influence on the emission properties. Additionally, *m*-carborane derivatives are significantly more fluorescent than their *o*- counterparts, reaching quantum yield values as high as 30.2%. Regarding the solid state emission, only stilbene-containing Ph-*o*-carborane derivatives, which showed very low fluorescence in solution, exhibited a notable PL emission in films attributed to the aggregation-induced emission. DFT calculations were performed to successfully complement the photoluminescence studies, supporting the experimentally observed photophysical behavior of the styrene and stilbene-containing carborane derivatives. In

Dalton Transactions Accepted Manuscript

View Article Online
DOI: 10.1039/C6DT04003A

conclusion, in this work is proved that it is possible to tailor the PL properties of the carborane-stilbene dyads by changing the C_c substituent and the carborane isomer.

Published on 13 December 2016. Downloaded by Instituto de Ciencia de Materiales de Barcelona (ICMAB) on 22/12/2016 09:59:23.

Dalton Transactions Accepted Manuscript

View Article Online
DOI: 10.1039/C6DT04003A

Published on 13 December 2016. Downloaded by Instituto de Ciencia de Materiales de Barcelona (ICMAB) on 22/12/2016 09:59:23.

Introduction

Dicarba-*closo*-dodecaboranes or simply carboranes ($C_2B_{10}H_{12}$), are electron-deficient boron clusters with three-dimensional electron delocalization inside the cage.[1, 2] The three isomers *ortho* (*o*-) (1,2-$C_2B_{10}H_{12}$), *meta* (*m*-) (1,7-$C_2B_{10}H_{12}$), and *para* (*p*-) (1,12-$C_2B_{10}H_{12}$) possess different electron-withdrawing capacity,[3] following the order: *o*- >> *m*- > *p*-,[4-6] attributed to a higher electronic delocalization and a lower distortion of the cage in the opposite order, *p*- ≈ *m*- >>> *o*-.[7] The electron-acceptor capacity of the *o*-carborane isomer has a key influence on the photoluminescence (PL) properties of a particular fluorophore when this is directly linked to the C_c atom, causing an efficient quenching of the fluorescence emission.[6, 8-10] This quenching takes place due to a rapid photoinduced electron-transfer (PET) process from the excited state S_1 of the fluorophore to the lower energy excited state S_x of the cluster, which inhibits the fluorescence emission of the fluorophore.[11] In 2007, our group reported the PL properties of *o*-carboranyl-functionalized large molecules based on poly(aryl-ether) derivatives,[12, 13] In these systems, the influence of the cluster (neutral *closo* clusters or their conceptually derived anionic *nido* clusters that are formally obtained by the removal of a B^+) on the fluorescence behavior was investigated. More recently, we developed a set of fluorescent dyads based on carboranes (see compounds **1-2** in Scheme 1) in which the styrene fragment is bound to at least one of the C_c atoms through a bridging methylene.[14] The study of the emission properties of these compounds revealed for the first time the significant role of the substituent linked to the adjacent C_c atom, demonstrating that if this substituent is an aromatic group, it can cause a quenching of the fluorescence. Another remarkable feature that has been previously reported for this kind of *o*-carborane derivatives is the significant enlargement of the cluster's C_c-C_c bond length.[15] This fact seems to be directly related

Dalton Transactions Accepted Manuscript

View Article Online
DOI: 10.1039/C6DT04003A

Published on 13 December 2016. Downloaded by Instituto de Ciencia de Materiales de Barcelona (ICMAB) on 22/12/2016 09:59:23.

to the PET process observed in the fluorophore bound to a C_c through the bridging methylene, when an aromatic group is linked to the adjacent C_c.[14, 16] The main objective of adding a terminal styrene moiety to the carborane cluster was to have a suitable group for further functionalization to develop conceptually different light-dependent macromolecules, like dendrimers or octasilsesquioxanes,[17, 18] as well as small fluorescent molecules.[16]

Due to the interest generated by the application of stilbene derivatives[19-21] in fields such as biomedicine,[22-25] electro-optic materials,[26] LEDs,[27] non-linear optics[28] among others; we aimed to develop new carborane-stilbene compounds from our previous styrene derivatives to study the influence of the C_c-substituted cluster on their photophysical properties. In a previous work, we synthesized stilbene-carborane triads in which *o*- or *m*-carborane clusters are linked to two stilbene units through a methylene spacer.[29] It was found that the presence of boron clusters preserves the PL behavior of the pristine stilbene in solution, but the exhibited fluorescence quantum yields were relatively low. These results revealed no CT contributions in the lowest excited state, since electronic communication is further diminished by the presence of the methylene spacer.

Keeping this in mind, in this work we have carried out the synthesis of novel fluorophores, in which one stilbene is bound through a methylene to one or two C_c-substituted *o*- and *m*-carborane clusters and studied the influence of these substituents and the cluster isomer on the PL properties. For this purpose, we started from the appropriate styrenyl-containing carboranes (**1**-**4**) that successfully reacted with an aryliodide or carboranyliodide (**5**-**8**) via Heck coupling reaction. Of special interest is to establish a correlation between the photophysical behavior of the styrene/stilbene unit and the electronic properties of the substituents at the second C_c (Me or Ph) for both the

Dalton Transactions Accepted Manuscript

View Article Online
DOI: 10.1039/C6DT04003A

Published on 13 December 2016. Downloaded by Instituto de Ciencia de Materiales de Barcelona (ICMAB) on 22/12/2016 09:59:23.

ortho- and *meta*- cluster isomers. To this end, the photoluminescence behavior of these compounds in both solution and solid state has been analyzed and its results are discussed and contrasted with ground-state DFT calculations.

Results and Discussion

Synthesis of compounds 3-16. The synthesis of substituted *o*- and *m*-carborane derivatives **3-8** has been achieved by nucleophilic substitution at the C_c atoms. Compounds **3** and **4** were prepared from 1-CH_3-1,7-*closo*-$C_2B_{10}H_{11}$ (Me-*m*-carborane) and 1-C_6H_5-1,7-*closo*-$C_2B_{10}H_{11}$ (Ph-*m*-carborane) in 67 and 40 % yield, respectively, following the same procedure used for their homologous *o*-carborane derivatives **1** and **2**.[14] Compounds **5-8** were obtained in moderate yields (55-73%) from the reaction of Me-*o*-carborane, Ph-*o*-carborane, Me-*m*-carborane and Ph-*m*-carborane with 1 equiv. of 4-iodobenzyl-bromide (see Experimental Section). From compounds **1-8**, compounds **9-12** were synthesized *via* Heck reaction,[30, 31] by reaction **1-4** with iodobenzene, whereas **13-16** were obtained from the reaction of **1-4** with **5-8** (Scheme 1). The Heck reaction from an unsaturated halogen and a terminal alkene in the presence of a base and Pd(0) catalysts is highly regioselective, producing *trans* coupling.[32] Two different sets of conditions were attempted for the Heck reaction to give **9-16** as *trans*-isomers (Table 1), but the best yields were achieved using [$Pd_2(dba)_3$], [Pd(t-$Bu_3P)_2$], NCy_2Me, 1,4-dioxane, at 100 ºC. Heck reactions were easily monitored by ^1H NMR, following the disappearance of the vinyl protons from **1-4**. Compounds **3-16** were characterized by using standard spectroscopic techniques: FT-IR, ^1H, ^{13}C and ^{11}B NMR, UV-Vis and fluorescence spectroscopies, MALDI-TOF MS, and elemental analysis (see ESI).

Dalton Transactions Accepted Manuscript

View Article Online
DOI: 10.1039/C6DT04003A

Published on 13 December 2016. Downloaded by Instituto de Ciencia de Materiales de Barcelona (ICMAB) on 22/12/2016 09:59:23.

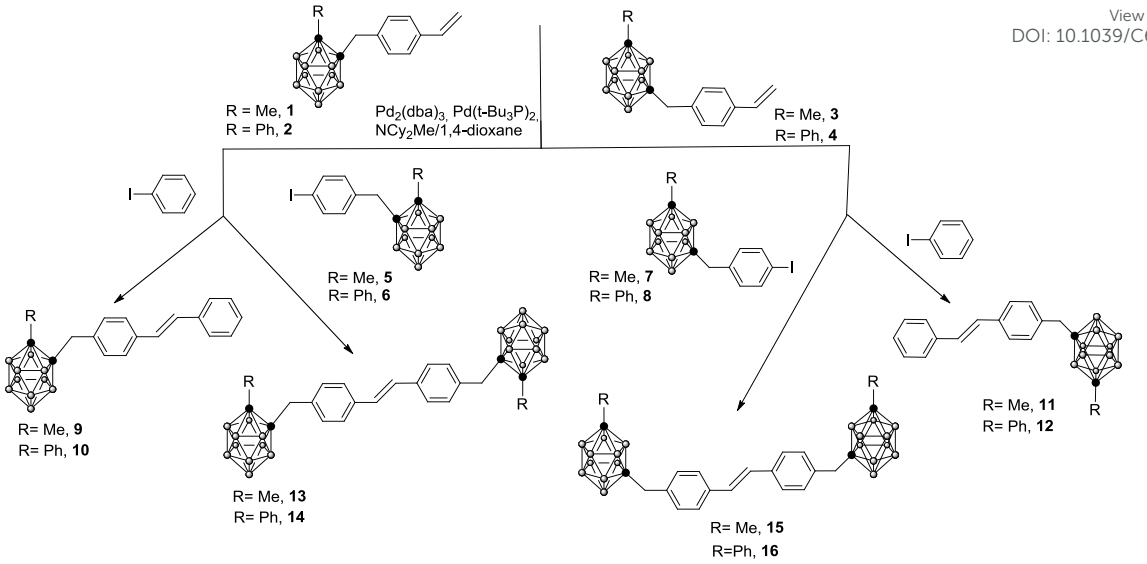

Scheme 1 Synthesis of stilbene-containing *o*- and *m*-carboranes **9**-**16**.

Table 1 Reaction yields for the stilbene-containing *o*- and *m*-carboranes **9-16**. [1]Conditions: $[PdCl_2(PPh_3)_2]$, CuI, 2,6-lutidine, DMF, 140 ºC.[33] [2]Conditions: $[Pd_2(dba)_3]$, $[Pd(t\text{-}Bu_3P)_2]$, NCy_2Me, 1,4-dioxane, 100 ºC.[34]

Compound	Time (h)[1]	Yield (%)[1]	Time (h)[2]	Yield (%)[2]
9	24	22	16	88
10	48	27	16	78
11	-	n/d	16	62
12	-	n/d	16	47
13	24	21	16	53
14	24	6	16	53
15	-	n/d	16	65
16	-	n/d	16	62

X-ray structures of 6, 7, 9, 12, 13, 14 and 15. Crystals of **6**, **7** and **9** suitable for X-ray analysis were obtained by slow evaporation of the corresponding compounds from solutions of Et_2O; crystals of **13** were grown by slow evaporation from a solution

Dalton Transactions Accepted Manuscript

View Article Online
DOI: 10.1039/C6DT04003A

of CH_2Cl_2. Crystals of **12, 14** and **15** were obtained by slow evaporation of the respective compounds from a mixture of THF/methanol (1:0.11) at 4 ºC. In Table S1 are listed some selected bond distances and Table 2 (see also Table S2) contains selected crystals data for these compounds. The molecular structures of stilbene-containing carboranes are presented in Fig. 1-5 (structures of compounds **6-7** in Fig. S1-S2).

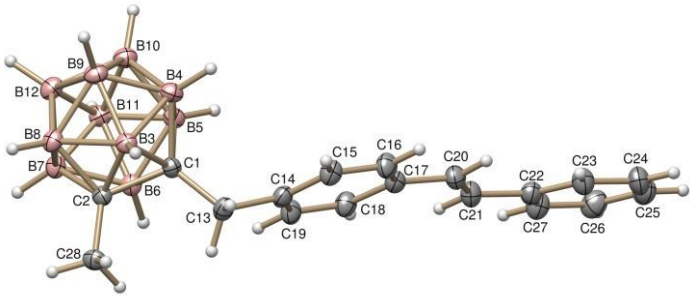

Fig. 1 ORTEP plot of the solid-state structure of **9**. Ellipsoids at 50% probability level.

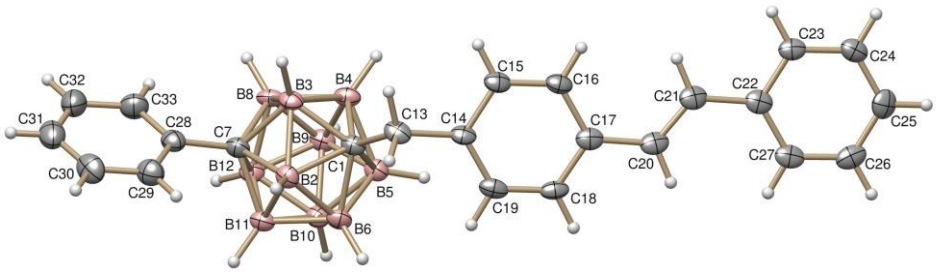

Fig. 2 ORTEP plot of the solid-state structure of **12.** Ellipsoids at 50% probability level.

Published on 13 December 2016. Downloaded by Instituto de Ciencia de Materiales de Barcelona (ICMAB) on 22/12/2016 09:59:23.

Dalton Transactions Accepted Manuscript

View Article Online
DOI: 10.1039/C6DT04003A

Published on 13 December 2016. Downloaded by Instituto de Ciencia de Materiales de Barcelona (ICMAB) on 22/12/2016 09:59:23.

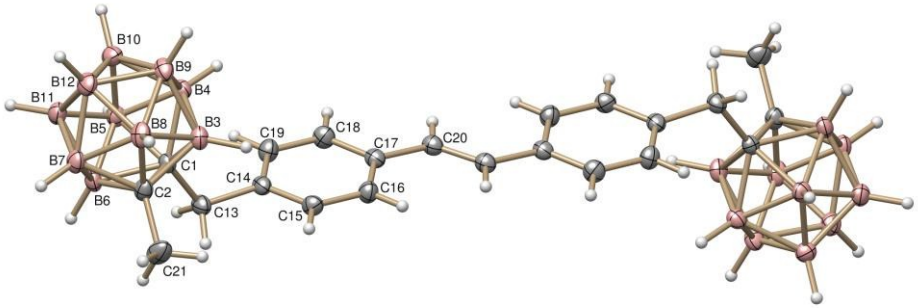

Fig. 3 ORTEP plot of the solid-state structure of **13.** Ellipsoids at 50% probability level.

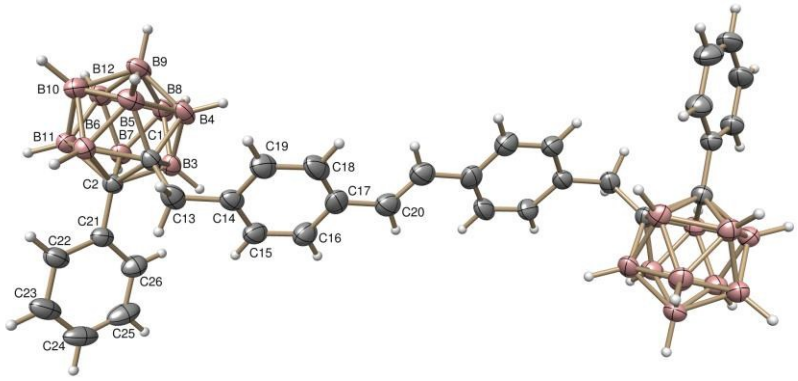

Fig. 4 ORTEP plot of the solid-state structure of **14.** Ellipsoids at 50% probability level.

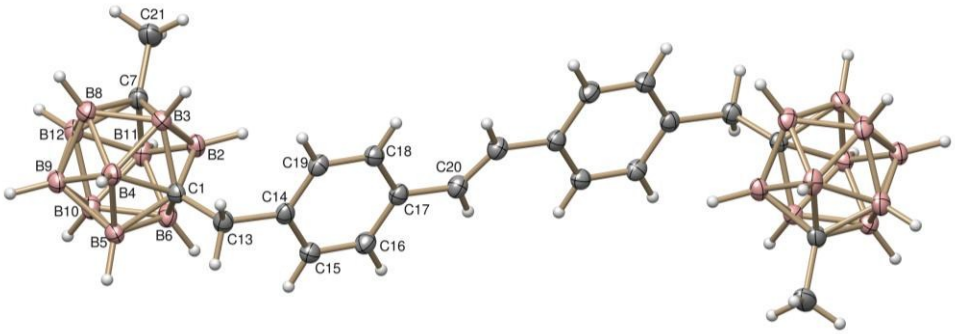

Fig. 5 ORTEP plot of the solid-state structure of **15.** Ellipsoids at 50% probability level.

Dalton Transactions Accepted Manuscript

View Article Online
DOI: 10.1039/C6DT04003A

Table 2 Selected crystallographic data for compounds **6**, **7**, **9** and **12-15.**

	6	**7**	**9**	**12**	**13**	**14**	**15**
empirical formula	$C_{15}H_{21}B_{10}I$	$C_{10}H_{19}B_{10}I$	$C_{18}H_{26}B_{10}$	$C_{23}H_{28}B_{10}$	$C_{22}H_{40}B_{20}$	$C_{32}H_{44}B_{20}$	$C_{22}H_{40}B_{20}$
fw	436.32	374.25	350.49	412.55	520.74	644.87	520.74
λ(Å)	0.71073	1.54184	0.71073	1.54178	0.71073	1.54184 Å	1.54184
cryst syst	Orthorhombic	Monoclinic	Monoclinic	Monoclinic	Monoclinic	Monoclinic	Monoclinic
space group	Pbca	$P2_1/n$	$P2_1/n$	$P2_1$	$P2_1/n$	$P2_1/c$	$P2_1/c$
a (Å)	8.0897(2)	7.75300(10)	11.9556(3)	11.4530(10)	6.6255(2)	14.4906(3)	12.0182(2)
b (Å)	21.1818(5)	17.9867(3)	7.5223(2)	7.2953(6)	28.5036(10)	12.2981(2)	12.79780(10)
c (Å)	22.1298(4)	11.8559(2)	45.0299(9)	27.575(2)	8.0673(3)	10.38440(10)	10.95890(10)
β (deg)	90	98.493(2)	92.6080(10)	97.317(8)	95.529(2)	91.1570(10)	113.436(2)
V (Å^3)	3792.04(15)	1635.19(4)	4045.51(17)	2285.2(3)	1516.43(9)	1850.19(5)	1546.50(4)
R1[a] ($I \geq 2\sigma$)	0.0226	0.0287	0.0541	0.0980	0.0487	0.0627	0.0430

[a] $R1 = \Sigma||F_o| - |F_c||/\Sigma|F_o|$.

In the crystal structures of compounds **6**, **7**, **12**, **13**, **14**, and **15**, weak interactions between carborane moieties are observed. Other secondary contacts (π-interactions, hydrogen bonds) between the substituents are more likely to be mainly van der Waals interactions. Additional data and figures of the packing for compounds **12-15** are given in the ESI.

Photophysical properties.

The photophysical behavior of the styrene-carboranyl derivatives **1-4** and stilbene-carboranyl derivatives **9-16** was determined by UV-Vis and fluorescence spectroscopy in CH_2Cl_2 (Fig. 6 and Table 3). Absorption spectra of compounds **1-4** show similar λ_{abs} maxima at around 255 nm due to the styrene group, which are very close to the values previously reported for **1-2** in CH_3CN.[14] Moreover, they show molar extinction coefficients in a close range, between $1.7 \cdot 10^4$ and $1.9 \cdot 10^4$ $M^{-1} \cdot cm^{-1}$,

Published on 13 December 2016. Downloaded by Instituto de Ciencia de Materiales de Barcelona (ICMAB) on 22/12/2016 09:59:23.

Dalton Transactions Accepted Manuscript

View Article Online
DOI: 10.1039/C6DT04003A

Published on 13 December 2016. Downloaded by Instituto de Ciencia de Materiales de Barcelona (ICMAB) on 22/12/2016 09:59:23.

independently of the isomer, *o*- or *m*-carborane. Compound **1** shows fluorescence emission maximum at around 309 nm with a quantum yield (Φ_F) of 15.4 %, whereas a quenching of the fluorescence was observed for **2** (Φ_F < 1 %), confirming the charge transfer (CT) process from the styrene moiety to the Ph-*o*-carborane cluster in the excited state, as was previously reported in CH_3CN solution.[14] Contrary to the *o*-carborane derivatives, for *m*-isomers no differences in the emission behavior between the Me-*m*-carborane derivative **3** and the Ph-*m*-carborane **4** were observed, which show emission maxima at 310 nm and higher Φ_F values of 29.1% and 30.2%, respectively. These results confirm that for *m*-carborane derivatives, the nature of the substituent attached to the second C_c does not make any influence on the emission intensity; nevertheless the bonding of both *m*-isomers to the styrene has produced an enhancement of the emission intensity compared to the pristine styrene.[35, 36]

For compounds **9**-**16**, the absorption maxima were expectedly red-shifted due to the increase of conjugation[37] after coupling reactions between their parent compounds **1**-**4** with iodobenzene or iodobenzyl-carboranyl derivatives **5**-**8** (Fig. 6). The vibronic structures of **9**-**16** include the three well-defined shoulders characteristic of stilbene, and the λ_{abs} values are in good agreement with reported absorption data of *trans*-stilbene derivatives.[38] Remarkably, it can be observed that compounds bearing two carborane clusters are 5 nm red-shifted with regards to those containing one cluster, which is the first dissimilarity in the photophysical behavior between both groups of compounds. Molar extinction coefficients for **9**-**16** are in the range $2.2\cdot10^4$-$3.2\cdot10^4$ $M^{-1}\cdot cm^{-1}$ (Table 3). In the emission spectra, the λ_{em} maxima for compounds with two carborane clusters, **13**-**16**, was red-shifted 6-16 nm with respect to compounds **9**-**12** that contain one cluster (Fig. 6 and Table 3). Stokes shifts collected in Table 3 (in nm) are in the 178571-243902 cm^{-1} range. *o*-Carborane derivatives **9** and **13** bearing a C_c-Me group displayed

Dalton Transactions Accepted Manuscript

View Article Online
DOI: 10.1039/C6DT04003A

Published on 13 December 2016. Downloaded by Instituto de Ciencia de Materiales de Barcelona (ICMAB) on 22/12/2016 09:59:23.

Φ_F values of 7.1 and 16.2%, respectively, which were higher to that of *trans*-stilbene (5% in methylcyclohexane),[39] suggesting that the grafting of Me-*o*-carborane to the stilbene group produces an important enhancement of the PL intensity. In contrast, compounds containing Ph-*o*-carborane **10** and **14** show much lower Φ_F values (2.4 and 2.9%, respectively), following the same trend previously observed for other Ph-*o*-carborane derivatives.[14, 16] When Me-*m*-carborane derivatives **11** and **15** were compared with their *o*-carborane counterparts **9** and **13**, it was observed that the former exhibited slightly higher Φ_F values (8.2 and 19.1%, respectively), very similar to their homologous Ph-*m*-carborane derivatives **12** and **16** (9.8 and 19.3% respectively). A general noteworthy feature of this set of compounds is the increase of the PL intensity for those stilbene bearing two carborane clusters with regards to those containing one, independently of the carborane isomer, with the exception of compounds **10** and **14**. In fact, emission intensities of **13**, **15** and **16** are more than twice of **9**, **11** and **12** (Table 3 and Fig. 6). It is reported that the presence of the bulky boron cages bound to conjugate systems should avoid π-π stacking formation in solution.[40] For our systems the hypothesis would be that the carborane clusters help to avoid the intermolecular π-π interactions, and additionally they may causes a decrease of the intramolecular rotation,[6] leading to higher emissions. In fact, it is reported the modification in the efficiency of PL deactivation by *trans-cis* photoisomerization of stilbene, by the presence of different substituents.[41] In any case, this phenomenon requires more understanding. To this aim more advances on the synthesis of new carboranyl-stilbene derivatives are underway.

Noticeably, for *o*-carborane derivatives with aromatic groups directly attached to the C_c, a particular correlation between Φ_F values and the C_c-C_c bond distance is observed: the larger the C_c-C_c distances, the lower the quantum yields in solution (Table 3).[16] The presence of aromatic groups causes an enlargement of the C_c-C_c distance due to the

Dalton Transactions Accepted Manuscript

View Article Online
DOI: 10.1039/C6DT04003A

Published on 13 December 2016. Downloaded by Instituto de Ciencia de Materiales de Barcelona (ICMAB) on 22/12/2016 09:59:23.

partial electronic filling of the cluster's LUMO located in σ* C_c-C_c,[15, 42] from the aromatic systems, generating a slightly positive charge that attracts the excited electron from the donor fragment to induce the quenching. In the present work, according to the data from the crystal structures, this phenomenon is also observed in the Ph-*o*-carborane derivatives **2** and **14**, as their C_c-C_c bond distances are considerably larger (0.28 and 0.26 Å, respectively) than those found for their counterparts with Me-*o*-carborane, **1** and **13** (Table 3). Simultaneously, Φ_F of **2** and **14** are much lower than those of **1** and **13**, fact that strongly supports this correlation and clearly confirms the important role of the substituent on the C_c-C_c distance, which is reflected on the PL properties. Unfortunately, the crystal structure of **10** was not determined, and its C_c-C_c distance could not be compared with the Me-*o*-carborane derivative **9** that has a very similar value to those of **1** and **13**. Prominently, **9** show larger emission intensity than **10** (Table 3).

Regarding the PL properties of compounds **9-16** in the solid state, it is noticed that only Ph-*o*-carboranes **10** and **14**, which are almost non-emissive in solution, exhibit a remarkable emission behavior in powder (Fig. S8 in ESI) and thin films (Fig. 7). Both compounds show a similar profile in solid state with a second red-shifted emission band with a maximum at λ_{em} ~ 540 nm and 520 nm respectively, attributed to the formation of an intermolecular excimer induced by aggregation effects.[43-45] To prove the aggregation-induced emission, solutions of compounds **10** and **14** in THF were treated with increasing amounts of water, leading to an aggregation of several molecules and inducing fluorescence emission in the same range of wavelength than for solids (Fig. 7). As it can be observed, for compound **10** the excimer emission is only visible when the water/THF ratio is higher than 95:5 (Fig. S9), whereas the excimer emission for **14** is detected with water/THF ratio higher than 99:1 (Fig. 7). This is due to the lower

Dalton Transactions Accepted Manuscript

View Article Online
DOI: 10.1039/C6DT04003A

solubility of compound **14** compared to **10**. Finally, the comparison of the absorption spectra of both **10** and **14** with their respective fluorescence excitation spectra show bands that overlap, may explain the excimer origin of this emission (Fig. S10).

These results reveal that for stilbene derivatives **9**-**16** the type of carborane isomer (*o*- or *m*-) plays a relevant role on the fluorescence in CH_2Cl_2 solution, so that *m*-carborane derivatives produce an enhancement of the fluorescence intensity, whereas *o*-carborane derivatives are regulated by electronic nature of the second substituent (Me or Ph). Hence the electronic nature of the substituent is a decisive factor in PL modulation in *o*-carborane derivatives; i.e. the Me group enhances the PL intensity, whereas the Ph group causes an important fluorescence decrease or even a total quenching.

Published on 13 December 2016. Downloaded by Instituto de Ciencia de Materiales de Barcelona (ICMAB) on 22/12/2016 09:59:23.

Dalton Transactions Accepted Manuscript

View Article Online
DOI: 10.1039/C6DT04003A

Table 3 Selected data of photophysical properties of compounds **1-4** and **9-16** in CH_2Cl_2. The C_c-C_c distances were determined from the crystal structures

Compound	Cluster	λ_{abs} (nm)	ε ($M^{-1}\cdot cm^{-1}$)	λ_{em} (nm)	Stokes shifts (nm)	Φ_F (λ_{exc}, nm)	d(C_c-C_c, Å)
1	*o*-Me	255	19720	309	54	0.154[a] (255)	1.684
2	*o*-Ph	255	18337	309	56	0.007[a] (255)	1.712
3	*m*-Me	255	19522	310	54	0.291[a] (255)	n/a
4	*m*-Ph	255	17078	310	56	0.302[a] (255)	n/a
9	*o*-Me	315	29070	352	43	0.071[b] (310)	1.680
10	*o*-Ph	315	26837	355	41	0.024[b] (310)	n/a
11	*m*-Me	315	27091	354	40	0.082[b] (310)	n/a
12	*m*-Ph	315	31078	354	42	0.098[b] (310)	n/a
13	2 *x* *o*-Me	320	28800	358	42	0.162[b] (310)	1.676
14	2 *x* *o*-Ph	320	22336	371	43	0.029[b] (310)	1.702
15	2 *x* *m*-Me	320	27764	361	43	0.191[b] (310)	n/a
16	2 *x* *m*-Ph	320	31547	361	43	0.193[b] (310)	n/a

[a]Styrene (Φ_F = 0.24 in cyclohexane)[35] or [b]Stilbene (Φ_F = 0.05 in methylcyclohexane)[39] were used as reference standards. n/a: data not available for unresolved crystal structures or not applicable for *meta* isomers.

Published on 13 December 2016. Downloaded by Instituto de Ciencia de Materiales de Barcelona (ICMAB) on 22/12/2016 09:59:23.

Dalton Transactions Accepted Manuscript

View Article Online
DOI: 10.1039/C6DT04003A

Published on 13 December 2016. Downloaded by Instituto de Ciencia de Materiales de Barcelona (ICMAB) on 22/12/2016 09:59:23.

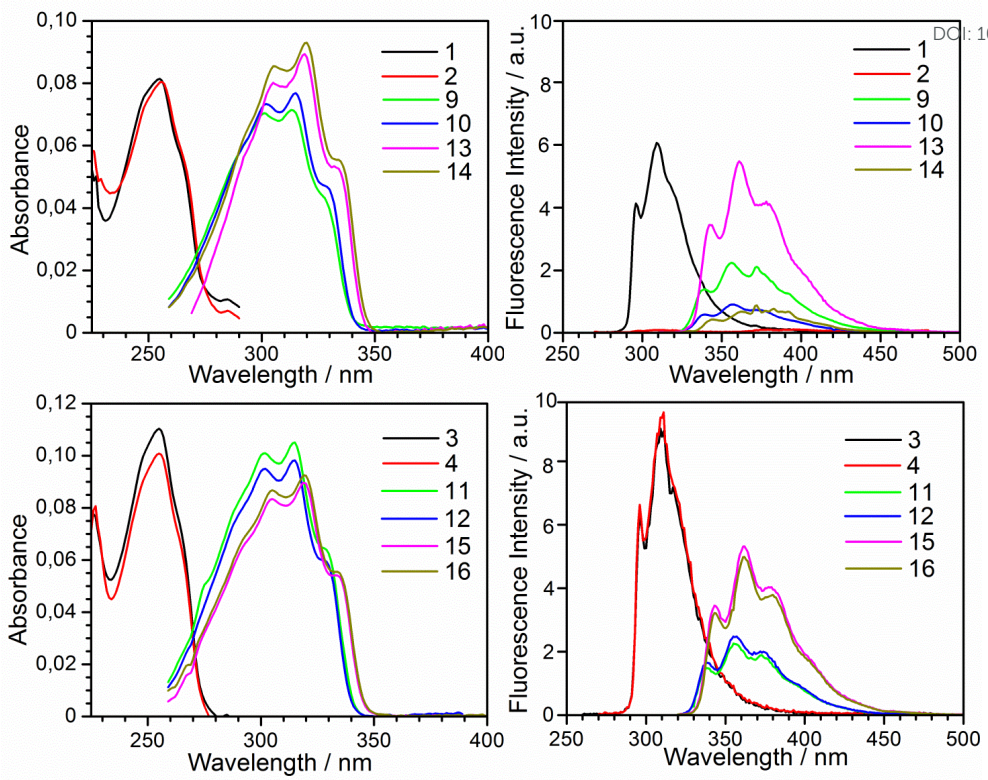

Fig. 6 Absorption and emission spectra (λ_{exc} = 255 nm for **1-4**; λ_{exc} = 310 nm for **9-16**) in CH_2Cl_2 for *ortho*-carborane derivatives **1-2**, **9-10** and **13-14** (top row) and *meta*-carborane derivatives **3-4**, **11-12** and **15-16** (bottom row).

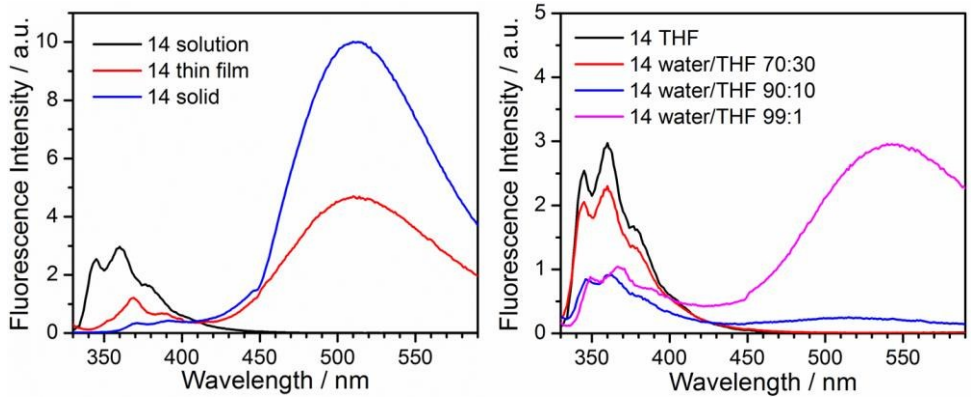

Fig. 7 Emission spectra of **14** in solution (THF), solid and thin film at λ_{exc} = 310 nm (left). Fluorescence emission of **14** in different THF:H_2O ratio at λ_{exc} = 320 nm (right).

Dalton Transactions Accepted Manuscript

View Article Online
DOI: 10.1039/C6DT04003A

Published on 13 December 2016. Downloaded by Instituto de Ciencia de Materiales de Barcelona (ICMAB) on 22/12/2016 09:59:23.

Theoretical interpretation.

As previously reported by our group,[14] the Ph-*o*-carborane derivative **2** experiences a strong quenching of the fluorescence due to a CT process, whereas the Me-*o*-carborane derivative **1** exhibits high fluorescence intensity, which was corroborated by theoretical calculations. In this work, their homologous *m*-carborane styrenyl compounds **3** and **4** have been examined and some predictions on emission properties for the counterpart *p*-carborane styrenyl (never synthesized because of lack of commercial supply) have been performed. Stilbene derivatives with one carborane cluster (**9**-**12**), and two carborane clusters (**13**-**16)** have also been analysed by DFT methods.

The molecular orbital composition analysis of compounds **1**-**4** and **9**-**16** determines where the most important molecular orbitals of the fluorophore moiety (HOMO/ LUMO) are located in the molecular structure. In our previous work,[14] such simple analysis was helpful to find out why the emission of the styrenyl moiety in Ph-*o*-carborane derivative **2** was quenched. As a rule of thumb, it can be established that if the LUMO is not placed in the fluorophore moiety, the fluorescence emission will be quenched. Calculations for all compounds (**1** and **2** have been remade to match the same level of theory used in this work to discard any inconsistency in occupation percentage) have been carried out, as well as the corresponding *p*-derivative for comparison. Fig. 8 shows the partial density of states (PDOS) of the optimized ground state structures of **1**-**4** and its *p*-isomer counterpart, according to the different fragments of the molecules.

Dalton Transactions Accepted Manuscript

View Article Online
DOI: 10.1039/C6DT04003A

Published on 13 December 2016. Downloaded by Instituto de Ciencia de Materiales de Barcelona (ICMAB) on 22/12/2016 09:59:23.

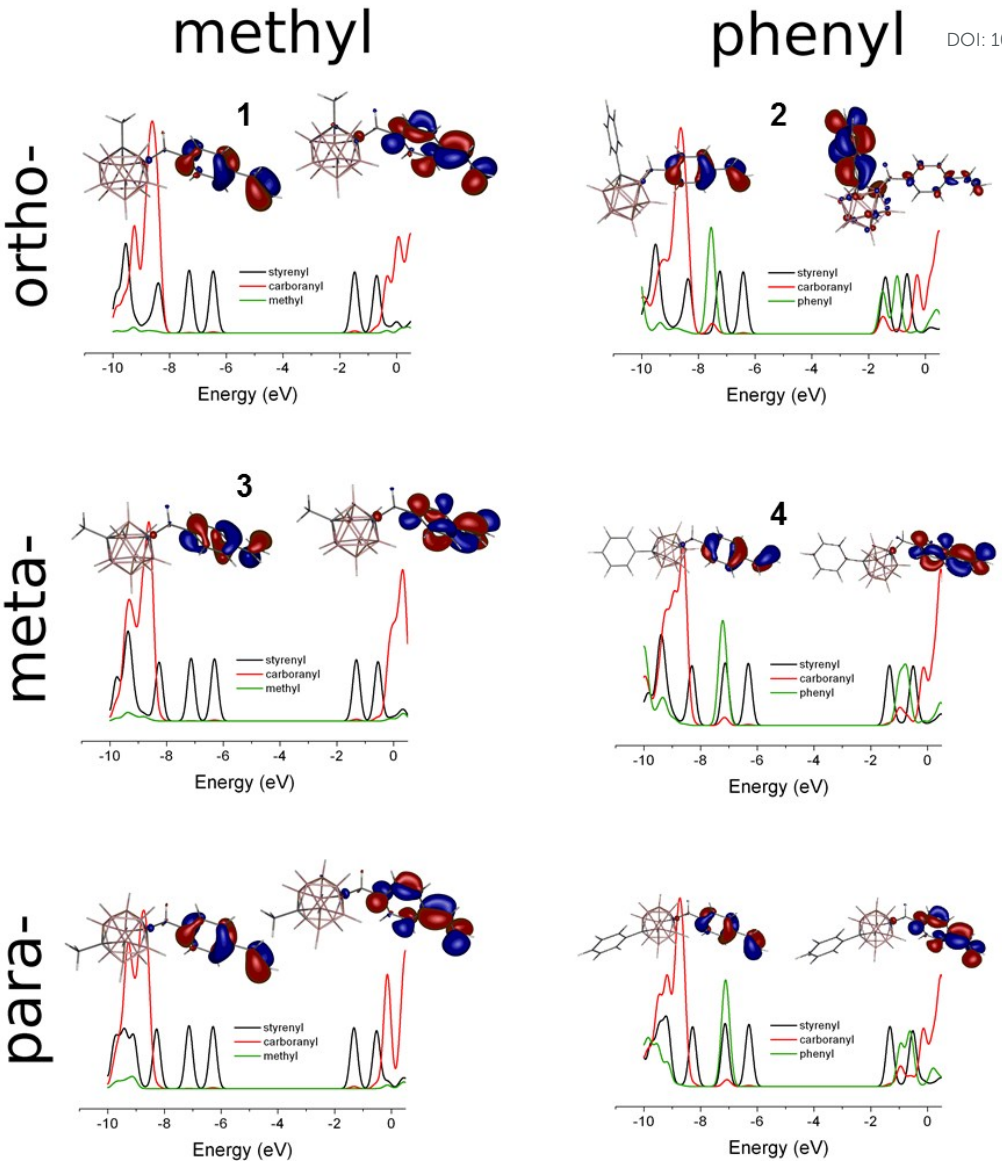

Fig. 8 PDOS and HOMO (left)/LUMO (right) density plots for styrene-containing carborane derivatives **1-4** and their theoretical *p*- counterparts. PDOS are shown in different colours for the different moieties; carboranyl (red), styrenyl moiety (black) and methyl or phenyl moiety attached in the remaining C_c (green).

Dalton Transactions Accepted Manuscript

View Article Online
DOI: 10.1039/C6DT04003A

Published on 13 December 2016. Downloaded by Instituto de Ciencia de Materiales de Barcelona (ICMAB) on 22/12/2016 09:59:23.

It can be observed that only **2** has a significant portion of the LUMO in the phenyl fragment, which implies a CT upon light excitation of the molecule continued by a radiationless de-excitation to the ground state. Importantly, this particular location of the LUMO is not observed for both Ph-*m*-carborane (**3**) and the *p*-isomer, which show low percentages of occupation on the carboranyl and substituent fragment, suggesting that the CT processes do not occur in these compounds and they should exhibit fluorescence emission, as experimentally observed. Table S4 collects the numerical percentage of occupation of these orbitals for the styrenyl compounds, which confirms the PL behaviour for compounds **3** and **4**. In fact, all styrenyl compounds but **2** exhibit fluorescence at room temperature in solution. Moreover, it must be highlighted that styrenyl derivatives have a calculated band gap of ~5 eV except compound **2**, for which is ~0.1 eV lower.

Ground-state DFT calculations were also performed to elucidate the energies of both HOMO and LUMO in all stilbene-containing derivatives **9-16**, and their PDOS plots are grouped in Fig. 9. A summary of the numerical percentage of occupation of LUMO orbitals for the stilbene-containing compounds is also available in the Table S4. From the theoretical point of view, contrary to styrene derivatives (Fig. 8), in which the HOMO and LUMO are different depending on the substituent, for stilbene derivatives minor differences can be observed on them. From Fig. 9 and it can be appreciate that both HOMO and LUMO are mainly located in the stilbene fragment for compounds **9-16**, suggesting that all of them should exhibit some fluorescence emission in solution. So that, it can be predicted that the fluorescence emission of stilbene-substitued Ph-*o*-carborane derivatives **10** and **14** should not be totally quenched by the CT process as was the case of compound **2**

Dalton Transactions Accepted Manuscript

View Article Online
DOI: 10.1039/C6DT04003A

This simple method analysis of the HOMO/LUMO composition using conventional ground state DFT optimizations only allows doing qualitative predictions about the fluorescence properties for these compounds. This method disregards any kind of quenching due to third party molecules (excimer formation) or another mechanism rather than its specific spatial structure conformation.

Published on 13 December 2016. Downloaded by Instituto de Ciencia de Materiales de Barcelona (ICMAB) on 22/12/2016 09:59:23.

Dalton Transactions Accepted Manuscript

View Article Online
DOI: 10.1039/C6DT04003A

Published on 13 December 2016. Downloaded by Instituto de Ciencia de Materiales de Barcelona (ICMAB) on 22/12/2016 09:59:23.

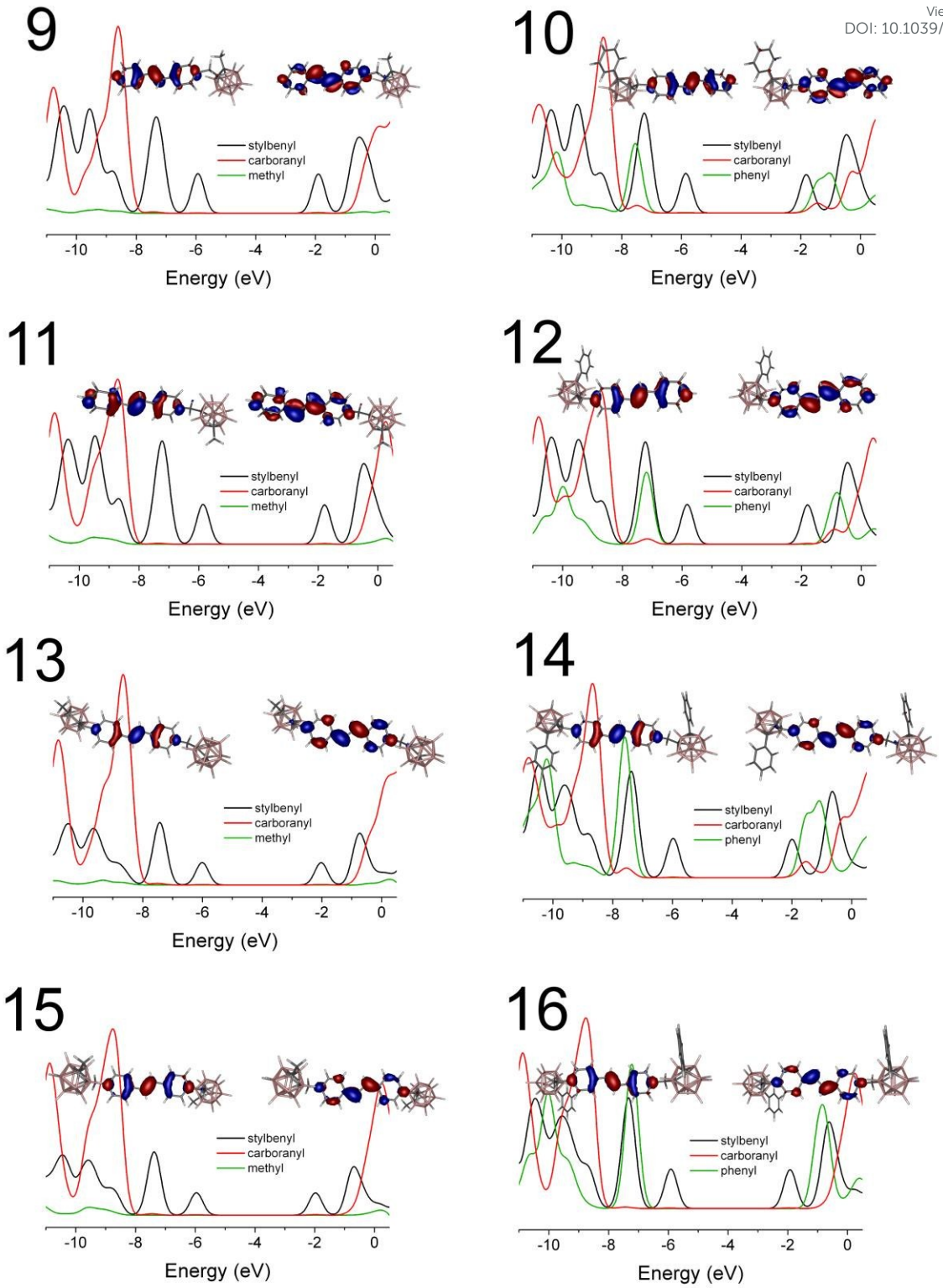

Fig. 9 PDOS and HOMO (left)/LUMO (right) density plots for stilbene-containing Me-*o*, Me-*m*, Ph-*o* and Ph-*m*-carborane derivatives **9-16**. PDOS are shown in different colours for the different moieties: carboranyl (red), stilbenyl moiety (black) and methyl or phenyl moiety attached in the remaining C_c (green).

Dalton Transactions Accepted Manuscript

View Article Online
DOI: 10.1039/C6DT04003A

Published on 13 December 2016. Downloaded by Instituto de Ciencia de Materiales de Barcelona (ICMAB) on 22/12/2016 09:59:23.

Conclusions

A new family of styrene and stilbene-containing *o*- and *m*-carborane dyads has been successfully synthesized and characterized. In all of them the fluorophore was bonded to the C_c via a methylene unit, which is a key point for their final photophysical properties. The crystal structures of seven compounds were analyzed by X-ray diffraction. Crystal structures of *o*-carborane derivatives revealed that those that contain a Ph group bonded to the C_c, **2** and **14**, have almost 0.3 Å longer C_c-C_c bond distances than their analogous **1** and **13** bearing a Me group. This phenomenon has been related with the fluorescence behavior, confirming that compounds **1** and **13** show considerably higher quantum yields than **2** and **14**, which has been attributed to a partial filling of the cluster's LUMO (σ^* C_c-C_c) from the phenyl group and giving rise to the fluorescence quenching. Concerning emission data, the main conclusions are the following: 1) Me-*o*-carborane derivatives show higher fluorescence quantum yields than their analogous Ph-*o*-carborane ones; 2) every stilbene derivative bearing *m*-carborane display fluorescence properties regardless of the second C_c substituent, with Φ_F values in the range 8.2-19.3 %; 3) a very small difference in the Φ_F values was observed between Me-*o*-carborane and Me-*m*-carborane derivatives that contain the same number of clusters, being almost the double for those compounds bearing two clusters; 4) large differences were detected when comparing the Φ_F values between Ph-*o*-carborane and Ph-*m*-carborane derivatives having one cluster: (2.4 %) and (16.2 %), respectively, or two clusters: (2.9 %) and (19.3 %), being particularly higher for the Ph-*m*-carborane derivatives; 5) remarkably, *m*-carborane derivatives bearing two clusters exhibit the highest fluorescence emission independently of the substituent at the second C_c (Me or Ph), confirming their low influence on the PL properties; 6) regarding the solid state emission, only Ph-*o*-carborane derivatives **10** and **14**, which were almost not fluorescent in solution, have

Dalton Transactions Accepted Manuscript

View Article Online
DOI: 10.1039/C6DT04003A

exhibited a notable PL emission in the solid state. Both compounds show an important emission red-shifted to around 540 nm attributed to the aggregation-induced excimer emission.

Published on 13 December 2016. Downloaded by Instituto de Ciencia de Materiales de Barcelona (ICMAB) on 22/12/2016 09:59:23.

Experimental

Instrumentation, X-Ray determination and **Calculations** details are available from the ESI.

Materials. All reactions were performed under an atmosphere of dinitrogen employing standard Schlenk techniques. Tetrahydrofuran and 1,4-dioxane were purchased from Merck and distilled from sodium benzophenone previously to use. DMF was purchased from Aldrich and distilled over anhydrous calcium oxide prior use. Commercial grade diethyl ether, ethyl acetate, hexane, chloroform and dichloromethane were used without further purification.[46] Compounds 1-C_6H_5-1,2-*closo*-$C_2B_{10}H_{11}$ and 1-CH_3-1,2-*closo*-$C_2B_{10}H_{11}$ were supplied by Katchem Ltd. (Prague) and used as received. 1-CH_3-1,7-*closo*-$C_2B_{10}H_{11}$ and 1-C_6H_5-1,7-*closo*-$C_2B_{10}H_{11}$ were obtained by thermal isomerization following the literature procedure.[47] Compounds **1, 2** and **5** were obtained using literature procedures.[14, 48] [$PdCl_2(PPh_3)_2$] was synthesized according to the literature.[49] 4-Vinylbenzyl chloride, *n*-BuLi solution (1.6 M in hexane), 4-iodobenzyl bromide, [$Pd_2(dba)_3$], [Pd(t-$Bu_3P)_2$], CuI and 2,6-lutidine were purchased from Aldrich. Iodobenzene was purchased from Alfa Aesar and NCy_2Me from Acros.

Compound 3.- A dry 25 mL round-bottomed flask equipped with a condenser and a magnetic stirring bar was charged under nitrogen with a solution of 1-CH_3-1,7-$C_2B_{10}H_{11}$ (0.520 g, 3.30 mmol) in THF (10 mL) at 0°C. Then, a solution of *n*BuLi 1.6M in

Dalton Transactions Accepted Manuscript

View Article Online
DOI: 10.1039/C6DT04003A

Published on 13 December 2016. Downloaded by Instituto de Ciencia de Materiales de Barcelona (ICMAB) on 22/12/2016 09:59:23.

hexanes (2.3 mL, 3.70 mmol) was added dropwise to the mixture, which was allowed to stir for 1 h at room temperature and cooled again at 0°C. Then, [4-(CH_2=CH)-C_6H_4-CH_2]Cl (0.57 mL, 3.60 mmol) was added rapidly to the mixture under vigorous stirring and it was reflux overnight. After that, the solvent was removed under vacuum and the oily residue was extracted with Et_2O (3x10 mL), transferred to a separating funnel and washed with H_2O (3 x 15 mL). The organic layer was dried over $MgSO_4$ and the volatiles were reduced under vacuum. The yellowish oil residue was purified by preparative layer chromatography (dichloromethane/hexane 1:1) to give **3** as colorless oil. Yield: 0.604 g, 67 %. **^{1}H NMR** ($CDCl_3$, TMS), δ(ppm): 7.38 (d, 2H, ^3J(H,H) = 9 Hz, C_6H_4), 7.09 (d, 2H, ^3J(H,H) = 9 Hz, C_6H_4), 6.73 (dd, 1H, ^3J(H,H) = 18 Hz, ^3J(H,H) = 9 Hz, C*H*=CH_2), 5.77 (d,1H, ^3J(H,H) = 18 Hz, CH=C*H*$_2$), 5.28 (d, 1H, ^3J(H,H) = 9 Hz, CH=C*H*$_2$), 3.19 (s, 2H, C*H*$_2$), 1.66 (s, 3H, C*H*$_3$); **^{1}H{^{11}B} NMR** ($CDCl_3$, TMS), δ(ppm): 7.38 (d, 2H, ^3J(H,H) = 6 Hz, C_6H_4), 7.09 (d, 2H, ^3J(H,H) = 9 Hz, C_6H_4), 6.73 (dd, 2H, ^3J(H,H) = 18 Hz, ^3J(H,H) = 9 Hz, 1H, C*H*=CH_2), 5.77 (d, 1H, ^3J(H,H) = 18 Hz, CH=C*H*$_2$), 5.28 (d, 1H, ^3J(H,H) = 9Hz, CH=C*H*$_2$), 3.20 (s, 2H, C*H*$_2$), 2.62 (s, 2H, B-*H*), 2.21 (s, 6H, B-*H*), 2.07 (s, 2H, B-*H*), 1.66 (s, 3H, C*H*$_3$); **^{11}B NMR** (CD_3COCD_3,BF_3·Et_2O), δ(ppm): -5.09 (d, 1B, ^1J(B,H) = 162 Hz), -6.78 (d, 1B, ^1J(B,H) = 224 Hz), -9.46 (d, 6B, ^1J(B,H) = 165 Hz), -11.43 (d, 2B, ^1J(B,H) = 188 Hz); **^{13}C{^{1}H} NMR** (CD_3COCD_3, TMS), δ(ppm): 136.89 (s, CH-*C*$_6$H$_4$), 136.79 (s, CH$_2$-*C*$_6$H$_4$), 136.47 (s, *C*H=CH_2), 130.17 (s, *C*$_6$H$_4$), 126.13 (s, *C*$_6$H$_4$), 113.45 (s, CH=*C*H$_2$), 77.28 (s, *C*$_c$-CH_2), 71.15 (s, *C*$_c$-CH_3), 42.09 (s, *C*H$_2$), 23.86 (s, C$_c$-*C*H$_3$); **ATR-IR** (ν_{max}/cm^{-1}): 3089 (w, C-H st), 3007 (w, C-H st), 2937 (w, C-H st), 2586 (s, B-H st); Anal. calcd. for $C_{12}H_{22}B_{10}$: C, 52.52; H, 8.08. Found: C, 52.80; H, 8.22.

Compound 4.- The procedure was the same as for **3**, but using a solution of 1-C_6H_5-1,7-$C_2B_{10}H_{11}$ (0.218 g, 0.99 mmol) in Et_2O (3 mL), *n*BuLi 1.6M in hexanes (0.68 mL,

Dalton Transactions Accepted Manuscript

View Article Online
DOI: 10.1039/C6DT04003A

Published on 13 December 2016. Downloaded by Instituto de Ciencia de Materiales de Barcelona (ICMAB) on 22/12/2016 09:59:23.

1.10 mmol) and a solution of [4-(CH_2=CH)-C_6H_4-CH_2]Cl (0.17 mL, 1.09 mmol) in THF (2 mL). After work-up, the yellowish oil residue was purified by preparative layer chromatography (dichloromethane/hexane 2:3) to give **4** as colorless oil. Yield: 0.133 g, 40 %. **^{1}H NMR** ($CDCl_3$, TMS), δ(ppm): 7.41-7.38 (m, 4H, C_6H_4 and C_6H_5), 7.30-7.25 (m, 3H, C_6H_5), 7.13 (d, 2H, ^3J(H,H) = 9 Hz, C_6H_4), 6.74 (dd, 1H, ^3J(H,H) = 18 Hz, ^3J(H,H) = 9 Hz, C*H*=CH_2), 5.79 (d, 1H, ^3J(H,H) = 18 Hz, CH=CH_2), 5.29 (d, 1H, ^3J(H,H) = 9 Hz, CH=CH_2), 3.29 (s, 2H, CH_2); **^{1}H{^{11}B} NMR** ($CDCl_3$, TMS), δ(ppm): 7.41-7.38 (m, 4H, C_6H_4 and C_6H_5), 7.30-7.25 (m, 3H, C_6H_5), 7.13 (d, 2H, ^3J(H,H) = 9 Hz, C_6H_4), 6.74 (dd, 2H, ^3J(H,H) = 18 Hz, ^3J(H,H) = 9 Hz, 1H, C*H*=CH_2), 5.79 (d, 1H, ^3J(H,H) = 18 Hz, CH=CH_2), 5.29 (d, 1H, ^3J(H,H) = 9 Hz, CH=CH_2), 3.29 (s, 2H, CH_2), 2.93 (s, 2H, B-*H*), 2.53 (s, 3H, B-*H*), 2.41 (s, 1H, B-*H*), 2.34 (s, 2H, B-*H*), 2.22 (s, 2H, B-*H*); **^{11}B NMR** ($CDCl_3$, BF_3·Et_2O), δ (ppm): -6.04 (d, 1B, ^1J(B,H) = 101 Hz), -6.83 (d, 1B, ^1J(B,H) = 111 Hz), -10.79 (d, 6B, ^1J(B,H) = 154 Hz), -13.63 (d, 2B, ^1J(B,H) = 175 Hz); **^{13}C{^{1}H} NMR** (CD_3COCD_3, TMS), δ (ppm): 136.88 (s, CH-C_6H_4), 136.40 (s, CH_2-C_6H_4), 136.33 (s, *C*H=CH_2), 135.28 (s, C_c-C_6H_5), 130.06 (s, C_6H_4), 128.54 (s, C_6H_5), 128.25 (s, C_6H_5), 127.78 (s, C_6H_5), 126.28 (s, C_6H_4), 114.08 (s, CH=*C*H_2), 78.15 (s, C_c-C_6H_5), 76.27 (s, C_c-CH_2), 42.93 (s, *C*H_2); **ATR-IR** (ν_{max}/cm^{-1}): 3029 (m, C-H st), 2928 (m, C-H st), 2854 (w, C-H st), 2585 (s, B-H st); Anal.Calcd. for $C_{17}H_{24}B_{10}$: C, 60.68; H, 7.19. Found: C, 60.92; H, 7.46.

Compound 5.- Following the literature procedure, compound **5** was obtained in 65% from 1-CH_3-1,2-$C_2B_{10}H_{11}$ (0.325 g, 2.06 mmol) and 4-iodobenzyl bromide (0.606 g, 1.98 mmol) in THF. **^{1}H NMR** ($CDCl_3$, TMS), δ(ppm): 7.70 (d, 2H, ^3J(H,H) = 9 Hz, C_6H_4), 6.95 (d, 2H, ^3J(H,H) = 9 Hz, C_6H_4), 3.42 (s, 2H, CH_2), 2.17 (s, 3H, CH_3); **^{1}H{^{11}B} NMR** ($CDCl_3$, TMS), δ(ppm): 7.70 (d, 2H, ^3J(H,H) = 9 Hz, C_6H_4), 6.95 (d, 2H, ^3J(H,H) = 9 Hz, C_6H_4), 3.42 (s, 2H, CH_2), 2.29 (s, 3H, B-*H*), 2.19 (s, 2H, B-*H*), 2.17 (s,

Dalton Transactions Accepted Manuscript

View Article Online
DOI: 10.1039/C6DT04003A

Published on 13 December 2016. Downloaded by Instituto de Ciencia de Materiales de Barcelona (ICMAB) on 22/12/2016 09:59:23.

3H, C*H*$_3$), 2.10 (s, 3H, B-*H*), 2.05 (s, 2H, B-*H*); **^{11}B NMR** ($CDCl_3$, $BF_3{\cdot}Et_2O$), δ(ppm): -4.15 (d, 1B, ^1J(B,H) = 150 Hz), -5.78 (d, 1B, ^1J(B,H) = 154 Hz), -9.91 (d, 4B, ^1J(B,H) = 100 Hz), -10.55 (d, 4B, ^1J(B,H) = 117 Hz); **^{13}C{^{1}H} NMR** ($CDCl_3$, TMS), δ(ppm): 137.79 (s, *C*$_6$H$_4$), 134.54 (s, *C*$_6$H$_4$), 132.15 (s, *C*$_6$H$_4$), 93.85 (s, *C*-I), 74.81 (s, *C*$_c$-CH$_3$), 40.75 (*C*H$_2$), 23.66 (s, C$_c$-*C*H$_3$); **ATR-IR** (ν_{max}/cm^{-1}): 3058 (w, C-H st), 2924 (m, C-H st), 2852 (w, C-H st), 2604 (s, B-H st), 2566 (s, B-H st); Anal.Calcd. for $C_{10}H_{19}B_{10}I$: C, 32.09; H, 5.12. Found: C, 33.12; H, 5.15.

Compound 6.- A dry 25 mL round-bottomed flask equipped with a magnetic stirring bar was charged under nitrogen with a solution of 1-C_6H_5-1,2-$C_2B_{10}H_{11}$ (200 g, 0.909 mmol) in THF (5 mL) , at 0°C. Then, a solution of *n*BuLi 1.6M in hexane (0.63 mL, 1 mmol) was added dropwise to the mixture, which was allowed to stir for 1 h at room temperature and then cooled to -84°C. After this, a solution of 4-iodobenzyl bromide (293 g, 0.937 mmol) in THF (5 mL) was added dropwise to the mixture under vigorous stirring and allowed to react at room temperature overnight. After that, the solvent was removed under vacuum and the orange residue was extracted with ethyl acetate (3 x 10 mL), transferred to a separating funnel and washed with a saturated aqueous solution of NaCl (3 x 10 mL). The organic layer was dried over $MgSO_4$ and the volatiles were reduced under vacuum. The orange oil residue was purified by preparative layer chromatography (ethyl acetate/hexane 15:85) leading to **6** as a colorless solid. Yield: 218 g, 55%. Crystal suitable for X-ray analysis was obtained by slow evaporation of a solution of **6** in Et_2O. **^{1}H NMR** ($CDCl_3$, TMS), δ(ppm): 7.72 (d, 2H, ^3J(H,H) = 6 Hz, C$_6$*H*$_5$), 7.58 (d, 2H, ^3J(H,H) = 9 Hz, C$_6$*H*$_4$), 7.45-7.55 (m, 3H, C$_6$*H*$_5$), 6.57 (d, 2H, ^3J(H,H) = 9 Hz, C$_6$*H*$_4$), 3.06 (s, 2H, C*H*$_2$); **^{1}H{^{11}B} NMR** ($CDCl_3$, TMS), δ(ppm): 7.72 (d, 2H, ^3J(H,H) = 6 Hz, C$_6$*H*$_5$), 7.58 (d, 2H, ^3J(H,H) = 9 Hz, C$_6$*H*$_4$), 7.45-7.55 (m, 3H, C$_6$*H*$_5$), 6.57 (d, 2H, ^3J(H,H) = 9 Hz, C$_6$*H*$_4$), 3.06 (s, 2H, C*H*$_2$), 2.71 (s, 2H, B-*H*), 2.42 (s,

Dalton Transactions Accepted Manuscript

View Article Online
DOI: 10.1039/C6DT04003A

Published on 13 December 2016. Downloaded by Instituto de Ciencia de Materiales de Barcelona (ICMAB) on 22/12/2016 09:59:23.

3H, B-*H*), 2.33 (s, 1H, B-*H*), 2.25 (s, 2H, B-*H*), 2.21 (s, 2H, B-*H*); **^{11}B NMR** ($CDCl_3$; $BF_3{\cdot}Et_2O$), δ(ppm): -3.55 (d, 2B, ^1J(B,H) = 143 Hz), -10.15 (d, 8B, ^1J(B,H) = 120 Hz); **^{13}C{^{1}H} NMR** ($CDCl_3$, TMS), δ(ppm): 137.52 (s, C_6H_4), 134.74 (s, C_6H_4), 131.92 (s, C_6H_4), 131.48 (s, C_6H_5), 130.97 (s, C_6H_5), 130.71 (s, C_6H_5), 129.13 (s, C_6H_5), 93.67 (s, *C*-I), 83.72 (s, C_c-C_6H_5), 81.36 (s, C_c-CH_2), 40.50 (s, CH_2); **ATR-IR** (ν_{max}/cm^{-1}): 3059 (w, C-H st), 2928 (w, C-H st), 2580 (s, B-H st), 2554 (s, B-H st); **MALDI-TOF-MS** (m/z): Calcd: 436.34. Found: 434.67 [M-2]; Anal. Calcd. for $C_{15}H_{21}B_{10}I$: C, 41.29; H, 4.85. Found: C, 41.33; H, 4.89.

Compound 7.- A dry 10 mL round-bottomed flask equipped with a magnetic stirring bar was charged under nitrogen with a solution of 1-CH_3-1,7-$C_2B_{10}H_{11}$ (0.200 g, 1.27 mmol) in THF (3.5 mL) at 0°C. Then, a solution of *n*BuLi 1.6M in hexanes (0.87 mL, 1.39 mmol) was added dropwise to the mixture, which was allowed to stir for 1 h at room temperature and cooled again at 0°C. Then, a solution of 4-iodobenzyl bromide (0.400 g, 1.31 mmol) in THF (3 mL) was added dropwise to the mixture under vigorous stirring. Then it was equilibrated at 0°C for 1 hour and then allowed to react at room temperature overnight. After that, the solvent was removed under vacuum and the residue was extracted with dichloromethane (3 x 10 mL), transferred to a separating funnel and washed with a saturated aqueous solution of NaCl (3 x 10 mL). The organic layer was dried over $MgSO_4$ and the volatiles were reduced under vacuum. The orange oil residue was purified by preparative layer chromatography (dichloromethane/hexane 15:85) to give **7** as a colorless solid. Yield: 0.346 g, 74 %. Crystal suitable for X-ray analysis was obtained by slow evaporation of a solution of **7** in Et_2O. **^{1}H NMR** ($CDCl_3$, TMS), δ(ppm): 7.67 (d, 2H, ^3J(H,H) = 9 Hz, C_6H_4), 6.87 (d, 2H, ^3J(H,H) = 9 Hz, C_6H_4), 3.15 (s, 2H, CH_2), 1.66 (s, 3H, CH_3); **^{1}H{^{11}B} NMR** ($CDCl_3$, TMS), δ(ppm): 7.67 (d, 2H, ^3J(H,H) = 9 Hz, C_6H_4), 6.87 (d, 2H, ^3J(H,H) = 9 Hz, C_6H_4), 3.15 (s, 2H, CH_2), 2.60

Dalton Transactions Accepted Manuscript

View Article Online
DOI: 10.1039/C6DT04003A

Published on 13 December 2016. Downloaded by Instituto de Ciencia de Materiales de Barcelona (ICMAB) on 22/12/2016 09:59:23.

(s, 2H, B-*H*), 2.27 (s, 1H, B-*H*), 2.18 (s, 5H, B-*H*), 2.07 (s, 2H, B-*H*),1.66 (s, 3H, C*H*$_3$); **^{11}B NMR** ($CDCl_3$, $BF_3{\cdot}Et_2O$), δ(ppm):-6.42 (d, 1B, ^1J(B,H) = 170 Hz), -8.25 (d, 1B, ^1J(B,H) = 241 Hz), -10.67 (d, 6B, ^1J(B,H) = 156 Hz), -13.33 (d, 2B, ^1J(B,H) = 191 Hz); **^{13}C{^{1}H} NMR** ($CDCl_3$, TMS), δ(ppm): 137.56 (s, C_6H_4), 136.50 (s, C_6H_4), 131.78 (s, C_6H_4), 93.16 (s, *C*-I), 75.98 (s, C_c-CH_2), 70.84 (s, C_c-CH_3), 42.42 (*C*H_2), 24.49, (s, C_c-*C*H_3); **ATR-IR** (ν_{max}/cm^{-1}): 3063 (w, C-H st), 2932 (m, C-H st), 2852 (w, C-H st), 2586 (s, B-H st); Anal.Calcd. for $C_{10}H_{19}B_{10}I$: C, 32.09; H, 5.12. Found: C, 32.32; H, 5.21.

Compound 8.- The procedure was the same as for **7**, but using a solution of 1- C_6H_5-1,7-$C_2B_{10}H_{11}$ (0.218 g, 0.99 mmol) in THF (3 mL), *n*BuLi 1.6M in hexanes (0.68 mL, 1.10 mmol) and a solution of 4-iodobenzyl bromide (0.315 g, 1.01 mmol) in THF (2 mL). After work-up, the orange oil residue was purified by preparative layer chromatography (ethyl acetate/hexane 10:90) and the white layer was extracted and purified again by preparative layer chromatography (dichloromethane/hexane 1:1) to give **8** as a colorless solid. Yield: 0.262 g, 60%. **^{1}H NMR** ($CDCl_3$, TMS), δ(ppm): 7.68 (d, 2H, ^3J(H,H) = 9 Hz, C_6H_4), 7.38 (d, 2H, ^3J(H,H) = 6 Hz, C_6H_5), 7.33-7.23 (m, 3H, C_6H_5), 6.90 (d, 2H, ^3J(H,H) = 9 Hz, C_6H_4), 3.24 (s, 2H, CH_2); **^{1}H{^{11}B} NMR** ($CDCl_3$, TMS), δ(ppm): 7.68 (d, 2H, ^3J(H,H) = 9 Hz, C_6H_4), 7.39 (d, 2H, ^3J(H,H) = 6 Hz, C_6H_5), 7.33-7.23 (m, 3H, C_6H_5), 6.90 (d, 2H, ^3J(H,H) = 9 Hz, C_6H_4), 3.24 (s, 2H, CH_2), 2.90 (s, 2H, B-*H*), 2.53 (s, 3H, B-*H*), 2.37 (s, 1H, B-*H*), 2.31 (s, 2H, B-*H*), 2.22 (s, 2H, B-*H*); **^{11}B NMR** ($CDCl_3$, $BF_3{\cdot}Et_2O$), δ(ppm): -6.16 (d, 2B, ^1J(B,H) = 104 Hz), -10.71 (d, 6B, ^1J(B,H) = 153 Hz), -13.62 (d, 2B, ^1J(B,H) = 175 Hz); **^{13}C{^{1}H} NMR** ($CDCl_3$, TMS), δ(ppm): 137.65 (s, C_6H_4), 136.40 (s, C_6H_4), 135.15 (s, C_6H_5), 131.81 (s, C_6H_4), 128.65 (s, C_6H_5), 128.33 (s, C_6H_5), 127.78 (s, C_6H_5), 93.32 (s, *C*-I), 78.37 (s, C_c-C_6H_5), 75.55 (s, C_c-CH_2), 42.88 (s, *C*H_2); **ATR-IR** (ν_{max}/cm^{-1}): 3055 (w, C-H st), 2925 (m, C-H st),

Dalton Transactions Accepted Manuscript

View Article Online
DOI: 10.1039/C6DT04003A

Published on 13 December 2016. Downloaded by Instituto de Ciencia de Materiales de Barcelona (ICMAB) on 22/12/2016 09:59:23.

2581 (s, B-H st);. Anal.Calcd. for $C_{15}H_{21}B_{10}I$: C, 41.29; H, 4.85. Found: C, 42.28; H, 5.09.

Compound 9.- A dry 5 mL round-bottomed flask equipped with a condenser and a magnetic stirring bar was charged under nitrogen with a solution of **1** (100 mg, 0.36 mmol), iodobenzene (82 mg, 0.40 mmol), [$Pd_2(dba)_3$] (3 mg, 0.004 mmol), [Pd(t-$Bu_3P)_2$] (3 mg, 0.006 mmol) and NCy_2Me (0.1 mL, 0.48 mmol) in 2 mL of 1,4-dioxane. The solution was stirred and refluxed at 100°C overnight. After that, the solution was filtered through 1 cm of Celite, which was washed with 10 mL of THF. The solvent mixture was removed in vacuo and then the residue was dissolved in 2 mL of THF. The solution was precipitated with 50 mL of methanol and filtered to give **9** as a white solid. Yield: 112 mg, 88 %. Crystal suitable for X-ray analysis was obtained by slow evaporation of a solution of **9** in Et_2O. **^{1}H NMR** ($CDCl_3$, TMS), δ (ppm): 7.57-7.50 (m, 4H, C_6H_5 + C_6H_4), 7.40 (dd, 2H, ^{3}J(H,H)= 9 Hz, ^{3}J(H,H)= 7.5 Hz, C_6H_5), 7.32 (d, 1H, ^{3}J(H,H)= 7.5 Hz, C_6H_5), 7.21 (d, 2H, ^{3}J(H,H)= 9 Hz, C_6H_4), 7.14 (d, 2H, ^{3}J(H,H)= 3 Hz, C*H*=C*H*), 3.49 (s, 2H, CH_2), 2.19 (s, 3H, -CH_3); **^{1}H{^{11}B} NMR** ($CDCl_3$, TMS), δ (ppm): 7.57-7.50 (m, 4H, C_6H_5 + C_6H_4), 7.40 (dd, 2H, ^{3}J(H,H)= 9 Hz, ^{3}J(H,H)= 7.5 Hz, C_6H_5), 7.32 (d, 1H, ^{3}J(H,H)= 7.5 Hz, C_6H_5), 7.21 (d, 2H, ^{3}J(H,H)= 9 Hz, C_6H_4), 7.14 (d, 2H, ^{3}J(H,H)= 3 Hz, C*H*=C*H*), 3.49 (s, 2H, CH_2), 2.32 (s, B-*H*), 2.27 (s, B-*H*), 2.19 (s, 3H, -CH_3), 2.12 (s, B-*H*). **^{11}B NMR** ($CDCl_3$, BF_3·Et_2O), δ (ppm): -4.22 (d, 1B, ^{1}J(B, H)= 143 Hz), -5.76 (d, 1B, ^{1}J(B,H)= 150 Hz), -10.47 (d, 8B, ^{1}J(B,H)= 132 Hz); **^{13}C{^{1}H} NMR** ($CDCl_3$, TMS), δ (ppm): 137.21 (s, C_6H_4), 134.08 (s, C_6H_4), 130.72 (s, C_6H_4), 129.51 (s, C_6H_5), 128.77 (s, CH=*C*H), 127.89 (s, *C*H=CH), 126.65 (s, C_6H_4 and C_6H_5), 74.65 (s, C_c-CH_3), 41.03 (s, *C*H_2), 23.71 (s, -*C*H_3); **ATR-IR** (ν_{max}/cm^{-1}): 3025 (w, C-H st), 2919 (m, C-H st), 2850 (w, C-H st), 2572 (s, B-H st); **MALDI-TOF-MS** (m/z):

Dalton Transactions Accepted Manuscript

View Article Online
DOI: 10.1039/C6DT04003A

Published on 13 December 2016. Downloaded by Instituto de Ciencia de Materiales de Barcelona (ICMAB) on 22/12/2016 09:59:23.

Calcd: 350.51. Found: 348.76 [M-2]; Anal. Calcd. for $C_{18}B_{10}H_{26}$: C, 61.68; H, 7.48. Found: C, 61.36; H, 7.47.

Compound 10.- The procedure was the same as for **9**, using **2** (100 mg, 0.30 mmol), iodobenzene (67 mg, 0.33 mmol), [$Pd_2(dba)_3$] (3 mg, 0.004 mmol), [$Pd(t\text{-}Bu_3P)_2$] (3 mg, 0.006 mmol) and NCy_2Me (0.1 mL, 0.48 mmol) in 2 mL of 1,4-dioxane. After workup compound **10** was obtained as a pure white solid. Yield: 95 mg, 78 %. **^{1}H NMR** ($CDCl_3$, TMS), δ (ppm): 7.75 (d, 2H, ^{3}J(H,H)= 9 Hz, C_6H_5), 7.55-7.46 (m, 5H, C_c-C_6H_5), 7.41-7.35 (m, 4H, , C_c-C_6H_5 + C_6H_5), 7.30 (d, 1H, ^{3}J(H,H)= 3 Hz, C_6H_5), 7.08 (d, 2H, ^{3}J(H,H)= 3 Hz, C*H*=C*H*), 6.83 (d, 2H, ^{3}J(H,H)= 6 Hz, C_6H_4), 3.11 (s, 2H, CH_2); **^{1}H{^{11}B} NMR** ($CDCl_3$, TMS), δ (ppm): 7.75 (d, 2H, ^{3}J(H,H)= 9 Hz, C_6H_5), 7.55-7.46 (m, 5H, C_c-C_6H_5), 7.41-7.35 (m, 4H, C_c-C_6H_5 + C_6H_5), 7.30 (d, 1H, ^{3}J(H,H)= 3 Hz, C_6H_5), 7.08 (d, 2H, ^{3}J(H,H)= 3 Hz, C*H*=C*H*), 6.83 (d, 2H, ^{3}J(H,H)= 6 Hz, C_6H_4), 3.11 (s, 2H, CH_2), 2.74 (s, B-H), 2.41 (s, B-H), 2.32 (s, B-H), 2.24 (s, B-H); **^{11}B NMR** ($CDCl_3$, $BF_3{\cdot}Et_2O$), δ (ppm): -3.68 (d, 2B, ^{1}J(B, H)= 146 Hz), -10.30 (d, 8B, ^{1}J(B,H)= 134 Hz); **^{13}C{^{1}H} NMR** ($CDCl_3$, TMS), δ (ppm): 137.17 (s, C_6H_4 and C_6H_5), 136.95 (s, CH_2-C_6H_4), 134.49(s, C_c-C_6H_5), 131.53 (s, C_c-C_6H_5), 130.87 (s, C_c-C_6H_5), 130.40 (s, C_c-C_6H_5), 129.26 (s, C_6H_5), 129.07 (s, C_6H_4), 128.72 (s, C_6H_5), 127.96 (s, CH=*C*H), 127.79 (s, *C*H=CH), 126.56 (s, C_6H_4), 126.41 (s, C_6H_5), 83.72 (s, C_c-C_6H_5), 82.06 (s, C_c-CH_2), 40.73 (s, CH_2); **ATR-IR** (ν_{max}/cm^{-1}): 2988 (m, C-H st), 2902 (m, C-H st), 2582 (s, B-H st), 2559 (s, B-H st); **MALDI-TOF-MS** (m/z): Calcd: 412.58. Found: 410.81 [M-2]. Anal. Calcd. for $C_{23}B_{10}H_{28}$: C, 66.96; H, 6.84. Found: C, 66.53; H, 7.05.

Compound 11.- The procedure was the same as for **9**, but using **3** (110 mg, 0.40 mmol), iodobenzene (84 mg, 0.42 mmol), [$Pd_2(dba)_3$] (3 mg, 0.004 mmol), [$Pd(t\text{-}Bu_3P)_2$] (3 mg, 0.006 mmol) and NCy_2Me (0.1 mL, 0.48 mmol) in 1,4-dioxane (2 mL). After workup compound **11** was obtained as a pure white solid. Yield: 87 mg, 62 %.**^{1}H**

Dalton Transactions Accepted Manuscript

View Article Online
DOI: 10.1039/C6DT04003A

Published on 13 December 2016. Downloaded by Instituto de Ciencia de Materiales de Barcelona (ICMAB) on 22/12/2016 09:59:23.

NMR ($CDCl_3$, TMS), δ(ppm): 7.55-7.47 (m, 4H, C_6H_5 + C_6H_4), 7.41-7.36 (m, 2H, C_6H_5), 7.30 (d, 1H, ^3J(H,H) = 6 Hz, C_6H_5), 7.13 (s, 2H, C*H*=C*H*), 7.12 (d, 2H, ^3J(H,H) = 6 Hz, C_6H_4), 3.22 (s, 2H, CH_2), 1.66 (s, 3H, CH_3); **^{1}H{^{11}B} NMR** ($CDCl_3$, TMS), δ(ppm): 7.55-7.47 (m, 4H, C_6H_5 + C_6H_4), 7.41-7.36 (m, 2H, C_6H_5), 7.30 (d, 1H,^3J(H,H) = 6 Hz, C_6H_5), 7.13 (s, 2H, C*H*=C*H*), 7.12 (d, 2H, ^3J(H,H) = 6 Hz, C_6H_4), 3.22 (s, 2H, CH_2), 2.64 (s, 2H, B-*H*), 2.22 (s, 6H, B-*H*), 2.08 (s, 2H, B-*H*), 1.66 (s, 3H, CH_3); **^{11}B NMR** ($CDCl_3$, $BF_3{\cdot}Et_2O$), δ(ppm): -6.52 (d, 1B, ^1J(B,H) = 155 Hz), -8.21 (d, 1B, ^1J(B,H) = 154 Hz), -10.77 (d, 6B, ^1J(B,H) = 151 Hz), -13.32 (d, 2B, ^1J(B,H) = 175 Hz); **^{13}C{^{1}H} NMR** ($CDCl_3$, TMS), δ (ppm): 137.27 (s, C_6H_4), 136.62 (s, C_6H_4), 136.40 (s, C_6H_5), 130.22 (s, C_6H_4), 129.00 (s, C_6H_5), 128.69 (s, C_6H_5), 128.14 (s, CH=*C*H), 127.69 (s, *C*H=CH), 126.51 (s, C_6H_4 and C_6H_5), 70.74 (s, C_c-CH_3), 42.72 (s, *C*H_2), 24.53 (s, *C*H_3); **ATR-IR** (ν_{max}/cm^{-1}): 3026 (m, C-H st), 2942 (m, C-H st), 2852 (w, C-H st), 2584 (s, B-H st);); **MALDI-TOF-MS** (m/z): Calcd: 350.51. Found: 351.34 [M+1]; Anal.Calcd. for $C_{18}H_{26}B_{10}$: C, 61.68; H, 7.48. Found: C, 61.73; H, 7.77.

Compound 12.- The procedure was the same as for **9**, but using **4** (90 mg, 0.27 mmol), iodobenzene (57 mg, 0.28 mmol), [$Pd_2(dba)_3$] (3 mg, 0.004 mmol), [$Pd(t\text{-}Bu_3P)_2$] (3 mg, 0.006 mmol) and NCy_2Me (0.1 mL, 0.48 mmol) in 1,4-dioxane (2 mL). After workup compound **12** was obtained as a pure white solid. Yield: 52 mg, 47 %. Crystal suitable for X-ray analysis was obtained by slow evaporation of **12** in a mixture THF/methanol (1:0.1) at 4 ºC. **^{1}H NMR** ($CDCl_3$, TMS), δ(ppm): 7.55-7.48 (m, 4H, C_6H_5 + C_6H_4), 7.41-7.37 (m, 4H, C_6H_5 + C_c-C_6H_5), 7.30 (d, 1H,^3J(H,H) = 6 Hz, C_6H_5), 7.28-7.24 (m, 3H, C_c-C_6H_5), 7.15 (d, 2H, ^3J(H,H) = 6 Hz, C_6H_4), 7.13 (s, 2H, C*H*=C*H*), 3.30 (s, 2H, CH_2); **^{1}H{^{11}B} NMR** ($CDCl_3$, TMS), δ(ppm): 7.55-7.48 (m, 4H, C_6H_5 + C_6H_4), 7.41-7.37 (m, 4H, C_6H_5 + C_c-C_6H_5), 7.30 (d, 1H, ^3J(H,H) = 6 Hz, C_6H_5), 7.28-7.24 (m, 3H, C_c-C_6H_5), 7.15 (d, 2H, ^3J(H,H) = 6 Hz, C_6H_4), 7.13 (s, 2H, C*H*=C*H*), 3.30 (s, 2H, CH_2),

Dalton Transactions Accepted Manuscript

View Article Online
DOI: 10.1039/C6DT04003A

Published on 13 December 2016. Downloaded by Instituto de Ciencia de Materiales de Barcelona (ICMAB) on 22/12/2016 09:59:23.

2.93 (s, 2H, B-*H*), 2.52 (s, 3H, B-*H*), 2.41 (s, 1H, B-*H*), 2.35 (s, 2H, B-*H*), 2.21 (s, 2H, B-*H*); **^{11}B NMR** ($CDCl_3$, $BF_3{\cdot}Et_2O$), δ(ppm): -6.24 (d, 2B, ^1J(B,H) = 65 Hz), -10.90 (d, 6B, ^1J(B,H) = 153 Hz), -13.73 (d, 2B, ^1J(B,H) = 170 Hz); **^{13}C{^{1}H} NMR** ($CDCl_3$, TMS), δ (ppm): 137.26 (s, C_6H_4), 136.69 (s, C_6H_4), 136.27 (s, C_6H_5), 135.29 (s, C_c-C_6H_5), 130.24 (s, C_6H_4), 129.05 (s, C_6H_5), 128.70 (s, C_6H_5), 128.57 (s, C_c-C_6H_5), 128.27 (C_c-C_6H_5), 128.11 (s, CH=*C*H), 127.79 (s, C_c-C_6H_5), 127.72 (s, *C*H=CH), 126.55 (s, C_6H_4 and C_6H_5), 78.11 (s, C_c-C_6H_5), 76.26 (s, C_c-CH_2), 42.95 (s, *C*H_2); **ATR-IR** (ν_{max}/cm^{-1}): 3029 (m, C-H st), 3922 (w, C-H st), 2850 (w, C-H st), 2585 (s, B-H st); **MALDI-TOF-MS** (m/z): Calcd: 412.58 Found: 412.42; Anal.Calcd. for $C_{23}H_{28}B_{10}$: C, 66.96; H, 6.84. Found: C, 66.63; H, 7.02.

Compound 13.- The procedure was the same as for **9**, but using **1** (90 mg, 0.27 mmol), **5** (136 mg, 0.36 mmol), [$Pd_2(dba)_3$] (5 mg, 0.006 mmol), [$Pd(t\text{-}Bu_3P)_2$] (5 mg, 0.01 mmol) and NCy_2Me (0.2 mL, 0.96 mmol) in 2 mL of 1,4-dioxane. After workup compound **13** was obtained as a pure white solid. Yield: 101 mg, 53 %. Crystal suitable for X-ray analysis was obtained by slow evaporation of a solution of **13** in CH_2Cl_2. **^{1}H NMR** ($CDCl_3$, TMS), δ (ppm): 7.51 (d, 4H, ^{3}J(H,H)= 9 Hz, C_6H_4), 7.21 (d, 4H, ^{3}J(H,H)= 9 Hz, C_6H_4), 7.12 (s, 4H, C*H*=C*H*), 3.49 (s, 4H, CH_2), 2.19 (s, 6H, -CH_3); **^{1}H{^{11}B} NMR** ($CDCl_3$, TMS), δ (ppm): 7.51 (d, 4H, ^{3}J(H,H)= 9 Hz, C_6H_4), 7.21 (d, 4H, ^{3}J(H,H)= 9 Hz, C_6H_4), 7.12 (s, 4H, C*H*=C*H*), 3.49 (s, 4H, CH_2), 2.30 (s, B-*H*), 2.23 (s, B-*H*), 2.19 (s, 6H, -CH_3), 2.11 (s, B-*H*); **^{11}B NMR** ($CDCl_3$, $BF_3{\cdot}Et_2O$), δ (ppm): -4.21 (d, 1B, ^{1}J(B, H)= 142 Hz), -5.71 (d, 1B, ^{1}J(B,H)= 148 Hz), -10.41 (d, 8B, ^{1}J(B,H)= 134 Hz); **^{13}C{^{1}H} NMR** ($CDCl_3$, TMS), δ (ppm): 136.94 (s, C_6H_4), 134.31 (s, C_6H_4), 130.59 (s, C_6H_4), 128.63 (s, *C*H=*C*H), 126.65 (s, C_6H_4), 74.79 (s, C_c-CH_3), 41.00 (s, *C*H_2), 23.75 (s, -*C*H_3); **ATR-IR** (ν_{max}/cm^{-1}): 3028 (w, C-H st), 2925 (m, C-H st), 2853 (w, C-H

Dalton Transactions Accepted Manuscript

View Article Online
DOI: 10.1039/C6DT04003A

Published on 13 December 2016. Downloaded by Instituto de Ciencia de Materiales de Barcelona (ICMAB) on 22/12/2016 09:59:23.

st), 2565 (s, B-H st); **MALDI-TOF-MS** (m/z): Calcd: 520.77. Found: 518.97 [M-2]; Anal. Calcd. for $C_{22}B_{20}H_{40}$: C, 50.74; H,7.74; Found: C, 50.64; H, 7.88.

Compound 14.- The procedure was the same as for **9**, but using **2** (77.5 mg, 0.23 mmol), **6** (100 mg, 0.23 mmol), [$Pd_2(dba)_3$] (5 mg, 0.006 mmol), [$Pd(t\text{-}Bu_3P)_2$] (5 mg, 0.01 mmol) and NCy_2Me (0.2 mL, 0.96 mmol) in 2 mL of 1,4-dioxane. After workup compound **14** was obtained as a pure white solid. Yield: 79 mg, 53%. Crystal suitable for X-ray analysis was obtained by slow evaporation of **14** in a mixture THF/methanol (1:0.1) at 4 ºC. **^{1}H NMR** ($CDCl_3$, TMS), δ (ppm): 7.74 (d, 4H, ^3J(H,H) = 9 Hz, C_6H_5), 7.61-7.47 (m, 6H, C_6H_5), 7.37 (d, 4H, 3J(H,H)= 9 Hz, C_6H_4), 7.03 (s, 2H, C*H*=C*H*), 6.82 (d, 4H, 3J(H,H)= 9 Hz, C_6H_4), 3.11 (s, 4H, CH_2); **^{1}H{^{11}B} NMR** ($CDCl_3$, TMS), δ (ppm): 7.74 (d, 4H, ^3J(H,H) = 9 Hz, C_6H_5), 7.61-7.47 (m, 6H, C_6H_5), 7.37 (d, 4H, ^{3}J(H,H)= 9 Hz, C_6H_4), 7.03 (s, 2H, C*H*=C*H*), 6.82 (d, 4H, ^{3}J(H,H)= 9 Hz, C_6H_4), 3.11 (s, 4H, CH_2), 2.75 (s, B-H), 2.41 (s, B-H), 2.24 (s, B-H); **^{11}B NMR** ($CDCl_3$, $BF_3{\cdot}Et_2O$), δ(ppm): -3.59 (d, 2B, ^{1}J(B, H)= 134 Hz), -10.12 (d, 8B, ^{1}J(B,H)= 125 Hz); **^{13}C{^{1}H} NMR** ($CDCl_3$, TMS), δ (ppm): 136.59 (s, *C*H=*C*H), 134.48 (s, C_6H_4), 131.25 (s, C_6H_5), 130.63 (s, C_6H_5), 130.14 (s, C_6H_4), 128.87 (s, C_6H_5), 128.17 (s, C_6H_5), 126.16 (s, C_6H_4), 83.58 (s, C_c-C_6H_5), 81.75 (C_c-CH_2) 40.34 (s, -CH_2-). **ATR-IR** (vmax/cm-1): 3027 (w, C-H st), 2919 (m, C-H st), 2851 (w, C-H st), 2565 (s, B-H st); **MALDI-TOF-MS** (m/z): Calcd: 644.99. Found: 643.11 [M-2]; Anal. Calcd. for $C_{32}B_{20}H_{44}$: C, 59.60; H, 6.88. Found: C, 59.62; H, 7.17.

Compound 15.- The procedure was the same as for **9**, but using **3** (100 mg, 0.36 mmol), **7** (73.3 mg, 0.36 mmol), [Pd_2dba_3] (5 mg, 0.006 mmol), [$Pd(t\text{-}Bu_3P)_2$] (5 mg, 0.01 mmol) and NCy_2Me (0.1 mL, 0.95 mmol) in 1,4-dioxane (2 mL). After work-up, compound **15** was obtained as a pure white solid. Yield: 90 mg, 65%. Crystal suitable for X-ray analysis was obtained by slow evaporation of **15** in a mixture THF/methanol

Dalton Transactions Accepted Manuscript

View Article Online
DOI: 10.1039/C6DT04003A

Published on 13 December 2016. Downloaded by Instituto de Ciencia de Materiales de Barcelona (ICMAB) on 22/12/2016 09:59:23.

(1:0.1) at 4 ºC. **^{1}H NMR** ($CDCl_3$, TMS), δ(ppm): 7.47 (d, 4H, ^{3}J(H,H) = 9 Hz, C_6H_4), 7.12 (d, 4H, ^{3}J(H,H) = 9 Hz, C_6H_4), 7.10 (s, 2H, C*H*=C*H*), 3.21 (s, 4H, CH_2), 1.66 (s, 6H, CH_3); **^{1}H{^{11}B} NMR** ($CDCl_3$, TMS), δ(ppm): 7.47 (d, 4H, ^{3}J(H,H) = 9 Hz, C_6H_4), 7.12 (d, 4H, ^{3}J(H,H) = 9 Hz, C_6H_4), 7.10 (s, 2H, C*H*=C*H*), 3.21 (s, 4H, CH_2), 2.64 (s, 4H, B-*H*), 2.22 (s, 12H, B-*H*), 2.08 (s, 4H, B-*H*), 1.66 (s, 6H, CH_3); **^{11}B NMR** ($CDCl_3$, $BF_3{\cdot}Et_2O$), δ(ppm): -6.45 (d, 2B, ^{1}J(B,H) = 147 Hz), -8.11 (d, 2B, ^{1}J(B,H) = 148 Hz), -10.66 (d, 12B, ^{1}J(B,H) = 152 Hz), -13.22 (d, 4B, ^{1}J(B,H) = 177 Hz); **^{13}C{^{1}H} NMR** ($CDCl_3$, TMS), δ(ppm): 136.52 (s, C_6H_4), 130.24 (s, C_6H_4), 128.42 (s, *C*H=*C*H), 126.50 (s, C_6H_4), 76.02 (s, C_c-CH_2), 70.79 (s, C_c-CH_3), 42.72 (s, CH_2), 24.52 (C_c-CH_3); **ATR-IR** (ν_{max}/cm^{-1}): 3024 (m, C-H st), 2938 (m, C-H st), 2589 (s, B-H st); **MALDI-TOF-MS** (m/z): Calcd: 520.77 Found: 521.65 [M+1]; Anal.Calcd. for $C_{22}H_{40}B_{20}$: C, 50.74; H, 7.74. Found: C, 50.86; H, 7.89.

Compound 16.- The procedure was the same as for **9**, but using **4** (68mg, 0.202mmol), **8** (88.2mg, 0.202mmol), [Pd_2dba_3] (3 mg, 0.003mmol), [Pd(t-$Bu_3P)_2$] (3 mg, 0.006mmol) and NCy_2Me (0.1 mL, 0.95 mmol) in 1,4-dioxane (2 mL). After work-up, compound **16** was obtained as a pure white solid. Yield: 81 mg, 62%. **^{1}H NMR** ($CDCl_3$, TMS), δ(ppm): 7.47 (d, 4H, ^{3}J(H,H) = 9 Hz, C_6H_4), 7.38 (d, 4H, ^{3}J(H,H) = 6 Hz, C_6H_5), 7.26-7.21 (m, 6H, C_6H_5), 7.12 (d, 4H, ^{3}J(H,H) = 9 Hz, C_6H_4), 7.10 (s, 2H, C*H*=C*H*), 3.29 (s, 4H, CH_2); **^{1}H{^{11}B} NMR** ($CDCl_3$, TMS), δ(ppm): 7.47 (d, 4H, ^{3}J(H,H) = 9 Hz, C_6H_4), 7.38 (d, 4H, ^{3}J(H,H) = 6 Hz, C_6H_5), 7.26-7.21 (m, 6H, C_6H_5), 7.12 (d, 4H, ^{3}J(H,H) = 9 Hz, C_6H_4), 7.10 (s, 2H, C*H*=C*H*), 3.29 (s, 4H, CH_2), 2.92 (s, 4H, B-*H*), 2.51 (s, 8H, B-*H*), 2.40 (s, 2H, B-*H*), 2.34 (s, 4H, B-*H*), 2.20 (s, 2H, B-*H*); **^{11}B NMR** ($CDCl_3$, $BF_3{\cdot}Et_2O$), δ(ppm): -6.01 (d, 4B, ^{1}J(B,H) = 156 Hz), -10.79 (d, 12B, ^{1}J(B,H) = 152 Hz), -13.50 (d, 4B, ^{1}J(B,H) = 196 Hz); **^{13}C{^{1}H} NMR** ($CDCl_3$, TMS), δ(ppm): 136.61 (s, C_6H_4), 136.39 (s, C_6H_4), 135.29 (s, C_6H_5), 130.24 (s, C_6H_4), 128.53 (s, C_6H_5),

Dalton Transactions Accepted Manuscript

View Article Online
DOI: 10.1039/C6DT04003A

128.44 (s, C_6H_5), 128.25 s, C_6H_5), 127.77 (s, *C*H=*C*H), 126.56 (s, C_6H_4), 79.57 (s, C_c-C_6H_5), 75.67 (s, C_c-CH_2), 42.96 (s, *C*H_2); **ATR-IR** (ν_{max}/cm^{-1}): 3024 (m, C-H st), 2928 (m, C-H st), 2854 (m, C-H st), 2592 (s, B-H st), 2557 (s, B-H st); **MALDI-TOF-MS** (m/z): Calcd: 644.91 Found: 645.73 [M+1]; Anal.Calcd. for $C_{32}H_{44}B_{20}$: C, 59.60; H, 6.88. Found: C, 59.70; H, 7.17.

Acknowledgements. This work has been supported by Ministerio de Economía y Competitividad, MINECO, (CTQ2013-44670-R and CTQ2013-41339-P), and Generalitat de Catalunya (2014/SGR/149). Theoretical calculations have been achieved using computers from the Centro Técnico de Informática del Consejo Superior de Investigaciones Ciéntificas (CTI-CSIC). ICMAB acknowledges financial support from the MINECO, through the "Severo Ochoa" Program for Centers of Excellence in R&D (SEV- 2015-0496).

Published on 13 December 2016. Downloaded by Instituto de Ciencia de Materiales de Barcelona (ICMAB) on 22/12/2016 09:59:23.

Dalton Transactions Accepted Manuscript

View Article Online
DOI: 10.1039/C6DT04003A

Published on 13 December 2016. Downloaded by Instituto de Ciencia de Materiales de Barcelona (ICMAB) on 22/12/2016 09:59:23.

References

1 J. Poater, M. Solà, C. Viñas and F. Teixidor, *Chem. Eur. J.*, 2013, **19**, 4372-4372.
2 J. Poater, M. Solà, C. Viñas and F. Teixidor, *Angew. Chem. Int. Ed.*, 2014, **53**, 12191-12195.
3 R. Núñez, P. Farràs, F. Teixidor, C. Viñas, R. Sillanpää and R. Kivekäs, *Angew. Chem. Int. Ed.*, 2006, **45**, 1270-1272.
4 N. Tsuboya, M. Lamrani, R. Hamasaki, M. Ito, M. Mitsuishi, T. Miyashita and Y. Yamamoto, *J. Mater. Chem.*, 2002, **12**, 2701-2705.
5 O. Crespo, M. C. Gimeno, A. Laguna, I. Ospino, G. Aullon and J. M. Oliva, *Dalton Trans.*, 2009, DOI: 10.1039/B820803D, 3807-3813.
6 L. Weber, J. Kahlert, R. Brockhinke, L. Böhling, A. Brockhinke, H.-G. Stammler, B. Neumann, R. A. Harder and M. A. Fox, *Chem. Eur. J.*, 2012, **18**, 8347-8357.
7 A. V. Okotrub, L. G. Bulusheva and V. V. Volkov, *J. Mol. Struct.*, 2000, **520**, 33-38.
8 K.-R. Wee, W.-S. Han, D. W. Cho, S. Kwon, C. Pac and S. O. Kang, *Angew. Chem. Int. Ed.*, 2012, **51**, 2677-2680.
9 L. Weber, J. Kahlert, R. Brockhinke, L. Bohling, J. Halama, A. Brockhinke, H.-G. Stammler, B. Neumann, C. Nervi, R. A. Harder and M. A. Fox, *Dalton Trans.*, 2013, **42**, 10982-10996.
10 P. A. Jelliss, in *Boron Science: New Technologies and Applications*, ed. N. S. Hosmane, CRC Press, Bosa Roca, 2011, ch. 15, pp. 355-382.
11 G. F. Jin, Y.-J. Cho, K.-R. Wee, S. A. Hong, I.-H. Suh, H.-J. Son, J.-D. Lee, W.-S. Han, D. W. Cho and S. O. Kang, *Dalton Trans.*, 2015, **44**, 2780-2787.
12 F. Lerouge, C. Viñas, F. Teixidor, R. Nuñez, A. Abreu, E. Xochitiotzi, R. Santillan and N. Farfan, *Dalton Trans.*, 2007, DOI: 10.1039/B618771D, 1898-1903.
13 F. Lerouge, A. Ferrer-Ugalde, C. Viñas, F. Teixidor, R. Sillanpaa, A. Abreu, E. Xochitiotzi, N. Farfan, R. Santillan and R. Nuñez, *Dalton Trans.*, 2011, **40**, 7541-7550.
14 A. Ferrer-Ugalde, E. J. Juárez-Pérez, F. Teixidor, C. Viñas, R. Sillanpää, E. Pérez-Inestrosa and R. Núñez, *Chem. Eur. J.*, 2012, **18**, 544-553.
15 J. M. Oliva, N. L. Allan, P. v. R. Schleyer, C. Viñas and F. Teixidor, *J. Am. Chem. Soc.*, 2005, **127**, 13538-13547.
16 A. Ferrer-Ugalde, A. González-Campo, C. Viñas, J. Rodríguez-Romero, R. Santillan, N. Farfán, R. Sillanpää, A. Sousa-Pedrares, R. Núñez and F. Teixidor, *Chem. Eur. J.*, 2014, **20**, 9940-9951.
17 A. González-Campo, A. Ferrer-Ugalde, C. Viñas, F. Teixidor, R. Sillanpää, J. Rodríguez-Romero, R. Santillan, N. Farfán and R. Núñez, *Chem. Eur. J.*, 2013, **19**, 6299-6312.
18 A. Ferrer-Ugalde, E. J. Juárez-Pérez, F. Teixidor, C. Viñas and R. Núñez, *Chem. Eur. J.*, 2013, **19**, 17021-17030.
19 B. A. Armitage and P. B. Berget, *Science*, 2008, **319**, 1195-1196.
20 A. S. Polo, M. K. Itokazu, K. M. Frin, A. O. de Toledo Patrocínio and N. Y. Murakami Iha, *Coord. Chem. Rev.*, 2006, **250**, 1669-1680.
21 K. Xiao, H.-J. Zhang, L.-J. Xuan, J. Zhang, Y.-M. Xu and D.-L. Bai, in *Series: Studies in Natural Products Chemistry*, ed. R. Atta ur, Elsevier, 2008, pp. 453-646.
22 D. He, W. Jian, X. Liu, H. Shen and S. Song, *J. Agric. Food. Chem.*, 2015, **63**, 1370-1377.
23 M. A. Romero, J. A. González-Delgado and J. F. Arteaga, *Nat. Prod. Comm.*, 2015, **10**, 1257-1262.
24 D. Ha, Q. Chen, T. Hung, U. Youn, T. Ngoc, P. Thuong, H. Kim, Y. Seong, B. Min and K. Bae, *Arch. Pharmacal Res.*, 2009, **32**, 177-183.
25 I. Chrząścik, *Crit. Rev. Anal. Chem.*, 2009, **39**, 70-80.
26 I. Fuks-Janczarek, R. Miedziński, E. Gondek, P. Szlachcic and I. V. Kityk, *J. Mater. Sci. Mater. Electron.*, 2008, **19**, 434-441.
27 Patent US8704215 B2, 2014.
28 V. Kundi and P. P. Thankachan, *Phys. Chem. Chem. Phys.*, 2015, **17**, 12299-12309.
29 J. Cabrera-González, C. Viñas, M. Haukka, S. Bhattacharyya, J. Gierschner and R. Núñez, *Chem. Eur. J.*, 2016, **22**, 13588-13598.

Dalton Transactions Accepted Manuscript

View Article Online
DOI: 10.1039/C6DT04003A

30 T. Mizoroki, K. Mori and A. Ozaki, *Bull. Chem. Soc. Jpn.*, 1971, **44**, 581-581.
31 R. F. Heck and J. P. Nolley, *J. Org. Chem.*, 1972, **37**, 2320-2322.
32 M. Oestreich, *The Mizoroki-Heck Reaction*, John Wiley & Sons, Münster, 2009.
33 P. Farràs, D. Olid-Britos, C. Viñas and F. Teixidor, *Eur. J. Inorg. Chem.*, 2011, **2011**, 2525-2532.
34 S. Sulaiman, J. Zhang, I. I. I. T. Goodson and R. M. Laine, *J. Mater. Chem.*, 2011, **21**, 11177-11187.
35 D. A. Condirston and J. D. Laposa, *Chem. Phys. Lett.*, 1979, **63**, 313-317.
36 P. M. Crosby and K. Salisbury, *J. Chem. Soc., Chem. Commun.*, 1975, DOI: 10.1039/C39750000477, 477-478.
37 B. Valeur, in *Molecular Fluorescence*, Wiley-VCH Verlag GmbH, Weinheim, 2001, ch. 4, pp. 54-56.
38 M. Aguiar, L. Akcelrud, M. Pinto, T. Atvars, F. Karasz and J. Saitiel, *J. Photosci.*, 2003, **10**, 149-156.
39 J. Saltiel and J. T. D'Agostino, *J. Am. Chem. Soc.*, 1972, **94**, 6445-6456.
40 B. P. Dash, R. Satapathy, E. R. Gaillard, J. A. Maguire and N. S. Hosmane, *J. Am. Chem. Soc.*, 2010, **132**, 6578-6587.
41 J. C. Roberts and J. A. Pincock, *J. Org. Chem.*, 2006, **71**, 1480-1492.
42 R. Kivekäs, R. Sillanpää, F. Teixidor, C. Viñas and R. Nuñez, *Acta Crystallogr.*, 1994, **C50**, 2027-2030.
43 Y. Hong, J. W. Y. Lam and B. Z. Tang, *Chem. Soc. Rev.*, 2011, **40**, 5361-5388.
44 M. Tominaga, H. Naito, Y. Morisaki and Y. Chujo, *New J. Chem.*, 2014, **38**, 5686-5690.
45 K. Kokado and Y. Chujo, *J. Org. Chem.*, 2011, **76**, 316-319.
46 R. Bernard, C. Barsu, P. L. Baldeck, C. Andraud, D. Cornu, J.-P. Scharff and P. Miele, *Chem. Commun.*, 2008, DOI: 10.1039/B804908D, 3765-3767.
47 M. F. Hawthorne, D. C. Young, P. M. Garrett, D. A. Owen, S. G. Schwerin, F. N. Tebbe and P. A. Wegner, *J. Am. Chem. Soc.*, 1968, **90**, 862-868.
48 E. Hao, B. Fabre, F. R. Fronczek and M. G. H. Vicente, *Chem. Mater.*, 2007, **19**, 6195-6205.
49 J. R. Blackburn, R. Nordberg, F. Stevie, R. G. Albridge and M. M. Jones, *Inorg. Chem.*, 1970, **9**, 2374-2376.

Published on 13 December 2016. Downloaded by Instituto de Ciencia de Materiales de Barcelona (ICMAB) on 22/12/2016 09:59:23.

Dalton Transactions Accepted Manuscript

View Article Online
DOI: 10.1039/C6DT04003A

Published on 13 December 2016. Downloaded by Instituto de Ciencia de Materiales de Barcelona (ICMAB) on 22/12/2016 09:59:23.

Graphical abstract

Carborane-stilbene dyads: influence of substituents and cluster isomers on the photoluminescence properties

A. Ferrer-Ugalde,[a#] J. Cabrera-González,[a] E. J. Juárez-Pérez,[a#] F. Teixidor,[a] E. Pérez-Inestrosa,[b,c] J. M. Montenegro,[b,c] R. Sillanpää,[d] M. Haukka and [d] R. Núñez*[a]

The fluorescence emission of stilbenes can be tailored by changing the substituent at the $C_{cluster}$ in *ortho*-carborane derivatives, whereas in the analogous *meta*-carboranes, the influence is much lower. Remarkably, incorporation of one or two carborane cages to the stilbene group can produce an important increase of its fluorescence intensity.

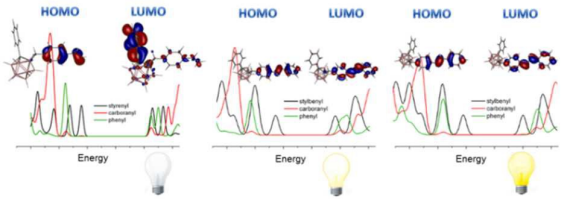

Dalton Transactions Accepted Manuscript